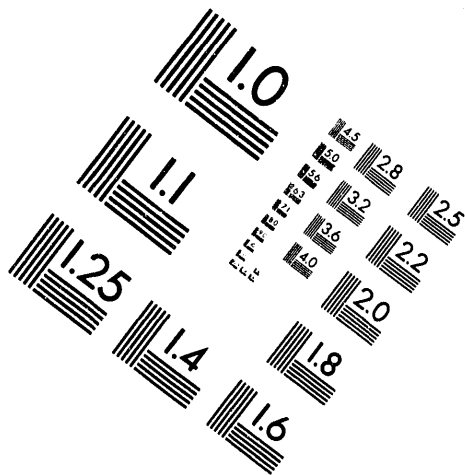
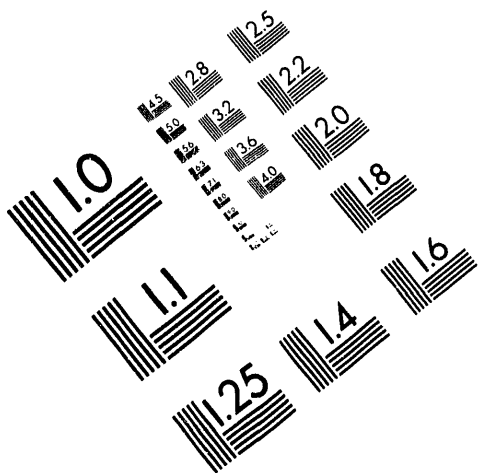




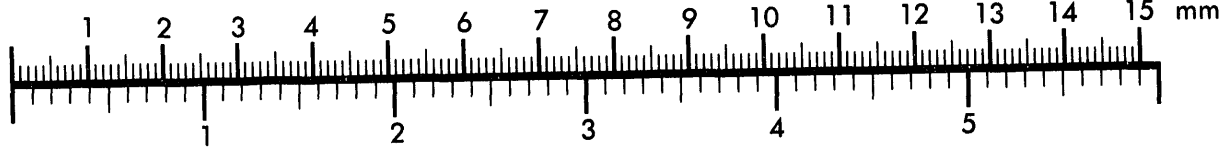
**AIM**

**Association for Information and Image Management**

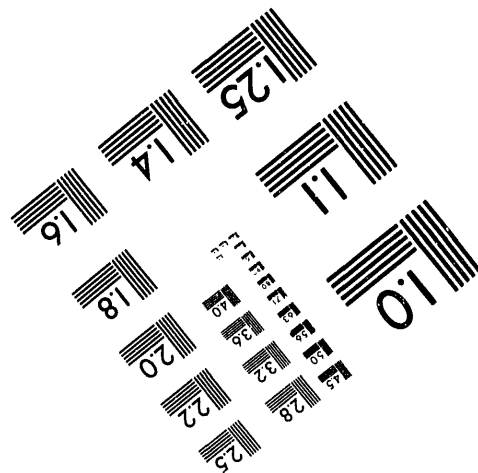
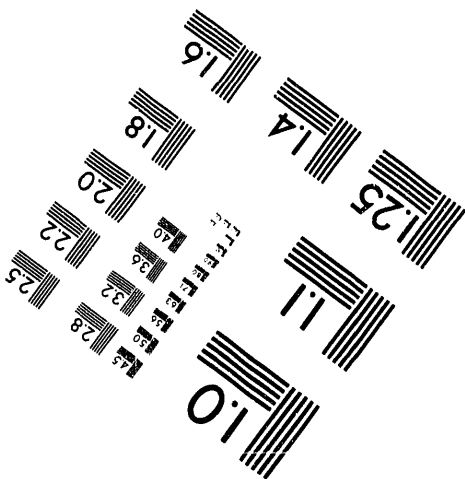
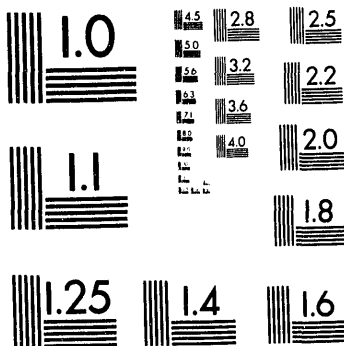
1100 Wayne Avenue, Suite 1100  
Silver Spring, Maryland 20910  
301/587-8202



Centimeter



Inches



MANUFACTURED TO AIM STANDARDS  
BY APPLIED IMAGE, INC.

**1 of 1**

MATHEMATICAL MODELING OF MIXER PUMP  
PERFORMANCE FOR AGITATION OF  
RADIOACTIVE SLURRIES IN ONE-MILLION-GALLON  
UNDERGROUND STORAGE TANKS AT HANFORD

J. A. Bamberger  
L. L. Eyster  
R. E. Dodge

April 1993

Prepared for  
the U.S. Department of Energy  
under Contract DE-AC06-76RLO 1830

Pacific Northwest Laboratory  
Richland, Washington 99352

**MASTER**

## SUMMARY

The objective of this work is to analyze the Hanford Waste Vitrification Project (HWVP) feed preparation tank mixing pump agitation design. This was accomplished by 1) reviewing mixing pump characteristics, 2) performing computer modeling of jet mixing and particulate material transport, 3) evaluating the propensity of the tank and mixing pump design to maintain particulate material in the tank in a uniformly mixed state, and 4) identifying important design parameters required to ensure optimum homogeneity and solids content during batch transfers.

These modeling investigations have shown that several parameters produce a profound effect on the ability of mixing pumps to maintain particulate in suspension and resuspend material that settles to the tank floor. These include:

- Particle Settling Velocity. Two particulate sizes and densities were investigated; these properties affect the particle settling velocity. Small, less dense particles are maintained in suspension more readily than large, more dense particles.
- Critical Shear Stress for Resuspension and Deposition. Critical shear stress for resuspension (deposition) denotes the shear stress above which (below which) material will be eroded from (deposited to) a bed load of material on the tank floor. Shear stress distribution is calculated at the tank floor along the path of the jet. Three critical shear stress assumptions were evaluated along the path of the jet: 1) greater than the maximum value, 2) less than the minimum value, and 3) between the maximum and minimum values. These assumptions correspond to situations where particulate material is 1) deposited (with no resuspension) at all positions along the jet path, 2) resuspended (with no deposition) at all positions along the jet path, and 3) resuspended over the portion of the jet path near the jet and deposited over the portion of the jet path away from the jet.
- Retrieval Pump Placement. Location of the retrieval pump can increase the uniformity of the feed stream concentration. This feature can be used to fine tune the uniformity of the feed stream.

These analyses have predicted mixer pump performance in the HWVP feed preparation tank based on a single, centered pump model. Results are extended to a six-pump design. The results show that the six-pump orientation has a good potential to provide a relatively uniform concentration throughout the tank, subject to certain limits on particle size and density. The greatest uncertainty in this work is in the estimation of critical shear stress for resuspension.

It would be extremely valuable if additional investigations were conducted to determine the critical shear stress for resuspension and deposition for settled solids for particulate types anticipated to be present in the HWVP feed preparation tanks.

## CONTENTS

SUMMARY . . . . .	iii
NOMENCLATURE . . . . .	xi
1.0 INTRODUCTION . . . . .	1.1
1.1 OBJECTIVES . . . . .	1.2
1.2 LIMITATIONS . . . . .	1.2
2.0 CONCLUSIONS AND RECOMMENDATIONS . . . . .	2.1
2.1 CONCLUSIONS . . . . .	2.1
2.1.1 Single-Pump, Flat-Tank-Floor Model . . . . .	2.1
2.1.2 Sloped-Floor Model . . . . .	2.2
2.1.3 Extension of Results to Six-Pump Design . . . . .	2.3
2.1.4 Retrieval Pump Operation . . . . .	2.4
2.1.5 Summary . . . . .	2.4
2.2 RECOMMENDATIONS . . . . .	2.5
3.0 MIXING THEORY AND FEED TANK AGITATION SYSTEM DEFINITION . . . . .	3.1
3.1 REVIEW OF MIXING LITERATURE . . . . .	3.1
3.1.1 Mechanical Mixing of Liquid/Liquid Mixtures . . . . .	3.1
3.1.2 Jet Mixing of Liquid/Liquid and Single-Phase Fluids . . . . .	3.4
3.1.3 Summary of Factors Affecting Mixing . . . . .	3.5
3.2 SYSTEM DEFINITION . . . . .	3.5
3.2.1 Geometry . . . . .	3.6
3.2.2 Pump Description and Operating Conditions . . . . .	3.8
3.3 DOUBLE-SHELL TANK WASTE PHYSICAL PROPERTIES . . . . .	3.8
3.4 MIXING PUMP CHARACTERISTICS . . . . .	3.11
3.4.1 Mobilizing Settled Solids . . . . .	3.11

3.4.2	Maintaining Solids in Suspension . . . . .	3.12
4.0	COMPUTER MODELING OF FEED TANK AGITATION SYSTEM . . . . .	4.1
4.1	OBJECTIVES OF COMPUTER MODELING . . . . .	4.1
4.2	BACKGROUND . . . . .	4.1
4.3	MODELING APPROACH . . . . .	4.2
4.3.1	Analysis Steps . . . . .	4.2
4.3.2	Assumptions . . . . .	4.3
4.3.3	Settling Velocity . . . . .	4.4
4.3.4	Single-Pump, Dual-Jet, Flat-Floor Model . . . . .	4.5
4.3.5	Resuspension Deposition Model . . . . .	4.5
4.3.6	Resuspension Deposition Shear Stress Data . . . . .	4.8
4.3.7	Effect of Sloped Floor . . . . .	4.9
4.3.8	Extension of Single Pump Modeling to Six-Pump Design Conditions . . . . .	4.9
4.4	RESULTS OF SINGLE-PUMP, FLAT-TANK FLOOR MODEL WITH PUMP ROTATION . . . . .	4.10
4.4.1	Computational Cases . . . . .	4.10
4.4.2	Hydrodynamic Results . . . . .	4.10
4.4.3	Solids Transport Results . . . . .	4.17
4.5	RESULTS OF SLOPED-FLOOR MODELING . . . . .	4.25
4.5.1	Geometric Considerations . . . . .	4.26
4.5.2	Description of Computer Modeling Approach . . . . .	4.29
4.5.3	Hydrodynamic Results . . . . .	4.30
4.6	EXTENSION OF RESULTS TO SIX-PUMP DESIGN . . . . .	4.31
4.6.1	Fluid Hydrodynamics of the Mixing Process . . . . .	4.32
4.6.2	Resuspension and Deposition . . . . .	4.34

4.6.3	Special Considerations of the Six-Pump Design . . . . .	4.36
5.0	OPERATIONAL AND DESIGN CONSIDERATIONS . . . . .	5.1
5.1	MAINTAINING UNIFORM CONCENTRATION IN THE HWVP PROCESS FEED	
STREAM	. . . . .	5.1
5.1.1	Mixing Pump Operation . . . . .	5.1
5.1.2	Retrieval Pump Operation . . . . .	5.3
5.2	DESIGN CONSIDERATIONS . . . . .	5.8
5.2.1	Physical Properties . . . . .	5.8
5.2.2	Geometric Parameters . . . . .	5.9
5.2.3	Dynamic Parameters . . . . .	5.11
REFERENCES	. . . . .	Ref.1

## FIGURES

1.1	Double-Shell Tank Waste Retrieval Equipment . . . . .	1.1
3.1	Schematic of the Six-Pump Agitation System Proposed for the HWVP Feed Preparation Tanks . . . . .	3.6
3.2	Planar View Schematic of Pump Locations . . . . .	3.7
3.3	Schematic of a Mixing Pump Expected to be Similar to Those Planned for HWVP Feed Preparation Tank Agitation . . . . .	3.9
4.1	Schematic of the Computational Domain of the Flat-Floor Model with a Single, Centrally Located Mixing Pump with Two Jets. . . . .	4.6
4.2	Comparison of the Velocity Profiles of a Floor Jet Computed for Fluid Depths of 9.1, 5.3, and 2.3 m (30, 17.3, and 7.6 ft) . . . . .	4.11
4.3	Flow Field (Left Half) and Wall Shear Stress Contours (Right Half) at the Floor of the Tank for Fluid Depth of 9.1 m (30 ft) . . . . .	4.14
4.4	Flow Field (Left Half) and Wall Shear Stress Contours (Right Half) at the Floor of the Tank for Fluid Depth of 5.3 m (17.3 ft) . . . . .	4.15
4.5	Flow Field (Left Half) and Wall Shear Stress Contours (Right Half) at the Floor of the Tank for Fluid Depth of 2.3 m (7.6 ft) . . . . .	4.16
4.6	Comparison of the Shear Stress Distribution Along the Jet Axis at the Floor of the Tank For Fluid Depths 9.1, 5.3, and 2.3 m (30, 17.3, and 7.6 ft). . . . .	4.17
4.7	Surface Representation of Solids Accumulation on the Floor (lbm/ft <sup>2</sup> ) for the Case of 70 $\mu$ m Particles, 9.1 m (30 ft) Fluid Depth, and a Low Critical Shear Stress [ $\tau_d = \tau_r = 11$ dyne/cm <sup>2</sup> (0.023 lbf/ft <sup>2</sup> )] Assumption . . . . .	4.19
4.8	Surface Representation of Solids Accumulation on the Floor (lbm/ft <sup>2</sup> ) for the Case of 70 $\mu$ m Particles, 9.1 m (30 ft) Fluid Depth, and a Medium Critical Shear Stress [ $\tau_d = \tau_r = 96$ dyne/cm <sup>2</sup> (0.200 lbf/ft <sup>2</sup> )] Assumption . . . . .	4.20
4.9	Surface Representation of Solids Accumulation on the Floor (lbm/ft <sup>2</sup> ) for the Case of 70 $\mu$ m Particles, 9.1 m (30 ft) Fluid Depth, and a High Critical Shear Stress [ $\tau_d = \tau_r = 358$ dyne/cm <sup>2</sup> (0.747 lbf/ft <sup>2</sup> )] Assumption . . . . .	4.21

4.10	Accumulation of Solids on Floor for Three Critical Stress Assumptions . . . . .	4.22
4.11	Accumulation of Solids on Floor for Three Critical Stress Assumptions . . . . .	4.23
4.12	Vertical Variation of Mass Fraction for Low Critical Shear Stress . . . . .	4.24
4.13	Vertical Variation of Mass Fraction for Medium Critical Shear Stress . . . . .	4.25
4.14	Vertical Variation of Mass Fraction for High Critical Shear Stress . . . . .	4.26
4.15	Schematic of Geometric Consideration of Mixing Jets Issuing from a Single Mixing Pump Offset from the Tank Center and Located above a Sloping Tank Floor . . . . .	4.26
4.16	Lines of Intersection of an Assumed Free Turbulent Jet with a Sloped Tank Floor (7 degree Jet Half Angle of Expansion and 3% Floor Slope) . . . . .	4.28
4.17	Comparison of Horizontal Velocity Profile at the Tank Centerline of a Flat Bottom and Three Sloped Bottom/Pump Location Combinations for a Pump Situated at a 6.4 m (21 ft) Radius . . . . .	4.31
4.18	Comparison of the Downward Slope Direction Turbulent Shear Stress Distribution on the Floor of the Tank Along the Axis of the Jets of a Flat Bottom and Three Sloped Bottom/Pump Location Combinations for a Pump Situated at a 6.4 m (21 ft) Radius . . . . .	4.32
4.19	Characteristic Velocity Profile for Three-Dimensional Flat Bottom Model . . . . .	4.32
4.20	Schematic of Deposition and Resuspension Areas on the Floor of a Six-Pump Design . . . . .	4.37
5.1	Constant Concentration Contours (-1%, Mean, +1%) for Homogeneity of 98% for 10- $\mu$ m Particulate at a Fluid Depth of 9.1 m (30 ft) . . . . .	5.2
5.2	Constant Concentration Contours (-2% and +2%) for Homogeneity of 96% for 10- $\mu$ m Particulate at a Fluid Depth of 9.1 m (30 ft) . . . . .	5.3
5.3	Constant Concentration Contours (-5% and +5%) for Homogeneity of 90% for 10- $\mu$ m Particulate at a Fluid Depth of 9.1 m (30 ft) . . . . .	5.4
5.4	Estimated Concentration Profiles as a Function of Height . . . . .	5.5
5.5	Optimum Retrieval Location as a Function of Inhomogeneity . . . . .	5.6

5.6	Variation in Feed Density as a Function of Remaining Feed Height . .	5.7
5.7	Schematic of the Four-Pump Agitation System . . . . .	5.10
5.8	Planar View of Four-Pump Configuration . . . . .	5.11

## TABLES

3.1	Pump Design Parameters . . . . .	3.8
3.2	Upper Limits of Physical Properties Used in Analysis . . . . .	3.10
4.1	Particle Settling Velocity Calculation . . . . .	4.5
4.2	Resuspension and Resuspendability Parameters . . . . .	4.8
4.3	Hydrodynamic Computation Cases . . . . .	4.11
4.4	Solids Transport (Long-Time Recycle) Computational Cases . . . . .	4.11
5.1	Proposed Homogeneity/Uniformity Specifications . . . . .	5.1

## NOMENCLATURE

$A_d$	area of particulate deposition
$A_j$	area swept by jet
$A_T$	total floor area
$D$	impeller blade diameter
$d_p$	particle diameter
DST	double-shell tank
$D_0$	jet nozzle diameter
ECR	effective cleaning radius
Fr	Froude number
$Fr_d$	densimetric Froude number
g	gravitational acceleration
H	tank height
$H_j$	height to which a jet will rise
HWVP	Hanford Waste Vitrification Project
m	species mass flux
N	impeller rotation rate
$N_{pj}$	relative density difference between jet and surrounding fluid
$N_T$	yield parameter
PNL	Pacific Northwest Laboratory
R	resuspendability of sediment species
Re	jet Reynolds number
$Re_i$	impeller Reynolds number
$Re_p$	particle Reynolds number
$t_d$	time interval between jet sweeps at a given location

$T_m$	mixing time
$U$	local jet velocity
$U_m$	jet centerline velocity
$U_0$	jet nozzle discharge velocity
$U_0 D_0$	nozzle discharge parameter
$V_s$	particle settling velocity
WHC	Westinghouse Hanford Company

### Greek Letters

$\alpha_{j,1/2}$	jet half angle of expansion
$\Theta$	jet angle with respect to the floor
$\mu_f$	fluid viscosity
$\Delta\rho$	density difference between jet and surrounding fluid
$\rho_f$	fluid density
$\rho_j$	jet density as it exits jet nozzle
$\rho_m$	mixture density
$\rho_s$	solids density
$\tau$	fluid shear stress
$\tau_d$	critical shear stress for deposition
$\tau_r$	critical shear stress for resuspension
$\tau_{ss}$	shear strength of sludge
$\Phi$	species mass fraction

## 1.0 INTRODUCTION

Oscillating jet mixing pumps with dual-opposed high velocity jets, as shown in Figure 1.1, are proposed for use in waste remediation and retrieval operations in double-shell tanks at Hanford. Analytical, experimental, and computational investigations to develop mixing pump operating strategies and to predict mixing pump performance are underway to support the Westinghouse Hanford Company (WHC) Double-Shell Tank Retrieval project and Waste Tank Safety program (Tank 101-SY Mitigation/Remediation). The information gained in these investigations is being applied to analyze the performance of the mixing pump configuration and the strategy for the Hanford Waste Vitrification Project (HWVP) feed tank mixing pump design and operation.

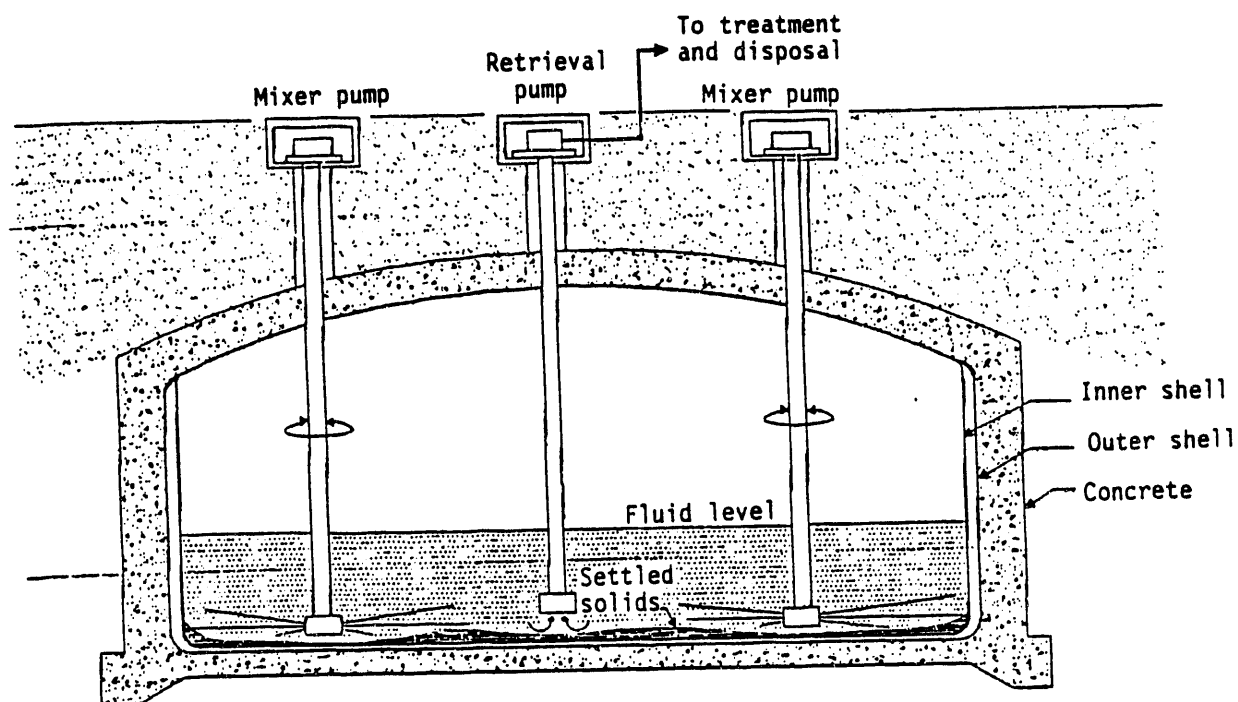


**FIGURE 1.1** Double-Shell Tank Waste Retrieval Equipment

## 1.1 OBJECTIVES

The objective of this work<sup>(a)</sup> is to project the performance of HWVP feed preparation tank mixing pump agitation. This is to be done by

- reviewing mixing pump characteristics
- performing computer modeling of jet mixing and particulate material transport
- evaluating the propensity of the tank and mixing pump design to maintain particulate material in the tank in a uniformly mixed state
- identifying important design parameters required to ensure optimum homogeneity and solids content during batch transfers.

## 1.2 LIMITATIONS

Limitations are inherent to any analysis because of uncertainties in defining the system and applicability of analytical tools. These limitations are listed below.

- Incomplete knowledge of the physical properties of the materials to be stored in the HWVP feed tank provides an uncertainty in the ability of the mixing pump to resuspend the particulate.
- The computational model being used for this analysis has not yet been developed to represent off-center mixing pumps that rotate. Therefore, a centrally located single mixer pump model that includes pump rotation is used as a basis for this analysis. A nonrotating pump model is used to investigate the sloped floor effects.
- The computational model of the free fluid surface at the liquid/air interface is nondeformable. At low liquid levels in the tank, the model does not represent the free surface (roiling) motion present directly above the jet.

The first of these limitations is related to uncertainties associated with deposition and resuspension of material on the tank floor. A critical shear stress model is used in the analysis. Initially this model requires constants for the critical shear stress for deposition, resuspendability of a

---

(a) The work was performed by Pacific Northwest Laboratory for Westinghouse Hanford Company. Pacific Northwest Laboratory is operated for the U.S. Department of Energy by Battelle Memorial Institute under Contract DE-AC06-76RLO 1830.

material, and critical shear stress for resuspension. Lack of knowledge of the physical characteristics of HWVP feed preparation tank contents limits applicability of resuspension constants obtained from literature and leads to an uncertainty that cannot be quantified. Uncertainty of deposition constants is reduced by making a conservative assumption that there is no hysteresis in the critical shear stress for deposition and resuspension.

The second limitation is not critical to this analysis. Results can be extended from the one-pump case to the six-pump case with some certainty through analysis of shear stress distribution along the axis of the jet.

The third limitation can only be addressed in a general way. While surface deformation is expected, especially at low liquid levels, its occurrence should be primarily related to surface effects (e.g., aerosol generation, bubble entrainment) and not to mixing in the liquid volume.

## 2.0 CONCLUSIONS AND RECOMMENDATIONS

Conclusions and recommendation that evolved from this analysis are presented.

### 2.1 CONCLUSIONS

The analysis was conducted in stages. Computations based on a single-pump, flat-tank-floor model defined hydrodynamics in the tank. This analysis was extended to a nonrotating sloped-floor model. Both were combined to develop the characteristics of a six-pump design. Separate considerations for retrieval were also addressed.

#### 2.1.1 Single-Pump, Flat-Tank-Floor Model

A centrally-located, rotationally-oscillatory, dual-jet mixing pump computer model was used to investigate hydrodynamics of the flow field and the effects of solids settling. For these investigations in the resuspension-deposition model, the critical shear stress for deposition ( $\tau_d$ ) was conservatively set equal to the critical shear stress for resuspension ( $\tau_r$ ).

- Three fluid depths [9.1, 5.3, and 2.3 m (30, 17.3 and 7.6 ft)] were investigated. Floor-jet characteristics change markedly for the lowest fluid depth case. The presence of the fluid surface limits the development of the floor jet by providing a hindrance to entrainment, and the jet flow that impinges upon the outer tank wall has greater tendency to move tangentially around the tank than to climb the outer wall. Buoyancy effects can be expected to exacerbate this problem in the event a non-uniformly mixed condition develops.
- The shear stress distributions along the axis of the jet for the three fluid depths calculated by the code are conservative. This was concluded because the shear stress predicted by the code was less than expected based on data from a correlation for a floor jet. Consequently the amount of deposited material that is predicted to be resuspended would be less than would occur in the tank.

Three critical shear stress assumptions (less than, equal to, and greater than the calculated floor shear stresses along the axis of the jet) were evaluated for 70 and 10  $\mu\text{m}$  particulate in 9.1-m (30-ft) depth fluid. The critical shear stress for resuspension of particulate material is of primary importance. If the critical shear stress for resuspension of settled material

is significantly less than the turbulent shear stress at every point on the tank floor, an equilibrium condition would exist wherein only a small fraction of the material in the tank would be on the floor at any given time (based on the jet oscillation rates and settling velocities used in these analyses).

The results show that

- For the low critical shear stress assumption, all material deposited on the floor between rotational sweeps of the jet is resuspended from the floor layer by the jet.
- For the equal critical shear stress assumption (in this case the critical shear stress that is assumed is greater than the minimum floor shear along the jet axis, but less than the maximum floor shear), material is resuspended over only a portion of the length of the jet axis where the turbulent shear stress of the jet is greater than the critical value for resuspension. Resuspended material is deposited further along the axis of the jet where the local turbulent shear stress of the jet is less than the critical value for deposition.
- For the high critical shear stress assumption, no material is entrained by resuspension and a relatively flat layer of material builds up on the floor. This layer could conceivably become rather thick over a long period of time.

### 2.1.2 Sloped-Floor Model

A sloped-floor model based on a single, stationary, dual-jet mixing pump, offset from the tank center was analyzed to investigate geometric intersection of an unconfined round free jet with a sloping tank floor and hydrodynamics of the jet and the shear stress distribution developed along the floor.

- Analysis of a jet with a 7 degree half angle of expansion indicates that there is sufficient overlap of the floor sweeping effect of the jets to well cover the whole floor of the HWVP feed preparation tank with six mixer pumps.
- Analysis of the offset stationary jet up-slope direction (shortest distance from pump to tank wall) and down-slope direction (longest distance from pump to tank wall) bounded the length over which jets from any single pump would traverse along the tank floor. The up-slope side shows increased shearing action, while the down-slope side shows decreased shearing action.

- For a six-pump configuration, the center of the tank has a greater propensity to accumulate particulate material because that is the region where the least shear stress exists for the resuspension of settled material in a six-pump configuration when the floor slopes downward toward the center.

### 2.1.3 Extension of Results to Six-Pump Design

The TEMPEST code limitation that a rotating pump could only be treated as centrally located requires that the results of the computer analysis be extrapolated to the six-pump design. Three areas were investigated: hydrodynamic mixing enhancements, physical processes of solid-liquid interactions, and special six-pump considerations.

- A single, centered mixing pump is capable of circulating 10- $\mu\text{m}$  diameter particulate throughout the tank (subject to uncertainty of critical shear stress for resuspension); six pumps (each operating at the design flow rate) would be expected to perform better than the single-pump model.
- For 70- $\mu\text{m}$  particulate with a specific gravity of three, potential exists for the jet to become buoyant (a forced plume) as particulate material settles between pump oscillations. A forced plume would tend to lift off the floor as a result of liquid becoming lighter as particles settle to the floor with time. If the jet becomes a forced plume and lifts off the floor, it becomes ineffective at resuspending settled material.
- The maximum distance that a jet must traverse in the six-jet configuration is 6.7 m (22 ft). This is less than the 9.9 m (37.5 ft) required for a single, centered mixer pump. Therefore, significantly larger average floor shear stresses would be expected for the six-pump orientation.
- Floor jets from adjacent pumps will necessarily intersect as the pumps rotate through a cycle. If the pumps are rotating synchronously and their jets are aligned, the ability of the floor jets to continuously sweep the entire tank floor may be impeded by the jets interfering with each other. To counter this potential, the pumps may be rotated asynchronously with varied rotation rates.
- Upon reaching the tank wall, the floor jet will be partially diverted up the wall and will be partially diverted azimuthally around the tank. Any portion diverted up will aid in mixing material resuspended from the floor. Any portion diverted azimuthally will carry material further towards a position where another jet from an adjacent pump will pick it up and move it back. This back and forth (washing machine) action should enhance mixing to maintain uniformity.

#### 2.1.4 Retrieval Pump Operation

There are two complementary methods to provide a uniform process feed:

- 1) maintaining uniform concentration throughout the tank via mixing pumps and
- 2) withdrawal of feed at a location within the tank that exhibits the specified concentration.

- Concentration profiles of settled solids as a function of elevation can be used to estimate the appropriate location of the retrieval pump inlet.

#### 2.1.5 Summary

These analytical and modeling investigations have shown that several parameters produce a profound effect on the ability of mixing pumps to resuspend settled particulate and maintain it in suspension.

- Particle Settling Velocity. Two particulate sizes and densities were investigated; these properties affect the particle settling velocity. Small, less dense particles are maintained in suspension more readily than large, more dense particles.
- Critical Shear Stress for Resuspension and Deposition. Three ranges, less than, equal to, and greater than the calculated floor shear stresses along the axis of the jet were evaluated. To resuspend particulate, the critical shear stress must be less than the floor shear stress or alternatively, the minimum shear stress along the axis of the jet must be greater than that required to resuspend settled material.
- Retrieval Pump Placement. Proper location of the retrieval pump inlet can enhance the uniformity of the retrieved feed stream. By locating the inlet at a tank location where the concentration remains uniform during mixer pump oscillation cycles and during retrieval as liquid level changes, uniformity of the feed stream is increased.

These analyses have predicted mixer pump performance in the HWVP feed preparation tank based on a single, centered pump model. The results show that the six-pump orientation has a good potential to provide a relatively uniform concentration throughout the tank. However, there is a potential for the fraction of material that is large particulate ( $>70 \mu\text{m}$ ) to settle to the tank floor and not be resuspended. The degree of feed stream uniformity can be improved by specific placement of the retrieval pump suction.

## 2.2 RECOMMENDATIONS

To provide a uniform feed stream from the HWVP feed preparation tanks it may be necessary to

- regulate the size of particulate placed within these tanks to less than 70  $\mu\text{m}$  in diameter through a pretreatment process. As diameter and density increase, the ability of the mixing pumps to resuspend the settled particulate decreases.
- use specific placement of the retrieval pump inlets to enhance the uniformity of the feed stream being withdrawn from the tank.

Confidence in the analysis of the ability of the jet to maintain uniformity in the tank would be enhanced by investigations to

- determine the critical shear stress for resuspension and deposition for settled solids that would occur in the HWVP feed preparation tanks
- optimize retrieval pump placement.<sup>(a)</sup>

---

(a) Retrieval investigations are planned to be conducted in the PNL Double-Shell Tank Retrieval project as a part of the 1/4-scale slurry uniformity investigations. The schedule for these tests has not been finalized.

### 3.0 MIXING THEORY AND FEED TANK AGITATION SYSTEM DEFINITION

Prior to defining the physical characteristics and design of the HWVP feed preparation system, a brief review of mixing literature is presented in Section 3.1. The HWVP feed preparation system is defined in Section 3.2. Physical properties of the feed are discussed in Section 3.3. Mixing pump characteristics are described in Section 3.4.

#### 3.1 REVIEW OF MIXING LITERATURE

The analysis presented in the slurry uniformity strategy plan (Bamberger, Liljegren, and Lowery 1993) was based on an extensive review of jet mixing literature. A summary of the results of that analysis follows. Tatterson (1991) uncovered no additional information in a brief review of tank mixing by jets.

When two fluids are placed in a tank, the concentration of a particular constituent will vary spatially. Stirring the liquids will reduce the concentration differences until the concentration in the tank approaches some constant value. The time required to reduce maximum concentration to a constant value depends upon the flow pattern induced by the mixer. This mixing time ( $T_m$ )<sup>(a)</sup> is also affected by flow velocity, turbulence, tank geometry, and fluid properties. Stirring in a vessel may be accomplished in two ways: mechanical agitators and jet mixers.

##### 3.1.1 Mechanical Mixing of Liquid/Liquid Mixtures

The mixing time required to reduce waste inhomogeneities in a tank using mechanical agitators has been experimentally determined in studies including those by Van de Vusse (1962), Kramers et al. (1953), Norwood and Metzner (1960), Marr (1959), and Fox and Gex (1956). These studies focused on the time required to reduce concentration differences in a tank to some arbitrarily small value. This time is referred to as the mixing time ( $T_m$ ). The results of these experiments are consistent and illustrate that the

---

(a) The mixing time is defined as the time required for an inhomogeneity introduced into a tank to be destroyed.

dimensionless mixing time in a tank is strongly affected by the Reynolds number when flow is laminar, but that dimensionless mixing time is unaffected by the Reynolds number when flow is turbulent. The experiments also indicate that the densimetric Froude number (ratio of mean kinetic energy to gravitational potential energy) is also important. Froude number appears in mixing correlations proposed by Van De Vusse (1962), Norwood and Metzner (1960), and Fox and Gex (1956). The dimensionless parameters governing mixing time in mechanically agitated vessels are expected to affect mixing achieved using jet mixers.

Van de Vusse (1955, 1962) measured the time required to mix two liquids of different densities that were initially stratified in the tank. A correlation to predict mixing times was developed as a function of impeller Reynolds number ( $Re_i$ ) and densimetric Froude number ( $Fr_d$ ).<sup>(a)</sup> The data were obtained using a propeller in an unbaffled vessel. Van de Vusse suggests that the effect of Reynolds number is negligible at impeller Reynolds numbers greater than 100,000.

Norwood and Metzner (1960) studied mixing of constant density fluids in baffled vessels using turbine agitators with six blades and obtained a correlation for dimensionless mixing time. Their analysis shows that the effect of Reynolds number on mixing time is unimportant above a blade Reynolds number of 1000. Fox and Gex (1956) also found results similar to those by Norwood and Metzner (1960).

The effect of both Froude number and Reynolds number can be justified physically. The Froude number describes the offsetting tendency of jet buoyancy and kinetic energy on the mixing achieved in a vessel and is consistently found to affect the mixing time in agitated vessels. The

---

(a)  $Re_i = (\rho_f D^2 N) / \mu_f$

where  $\rho_f$  is the density of the mixed liquid,  $D$  is the impeller blade diameter,  $N$  is the impeller rotation rate, and  $\mu_f$  is the fluid viscosity.

$$Fr_d = (\rho_f N^2 D^2) / (\Delta\rho g H)$$

where  $\Delta\rho$  is the density difference between the two fluids,  $g$  is the acceleration caused by gravity, and  $H$  is the fluid height.

quantitative effect of varying Froude number appears to depend on the density difference between the fluids. When the jet is more dense than the surrounding fluid, dimensionless mixing time decreases with an increasing densimetric Froude number. When the jet is neutrally buoyant, the mixing time increases with an increasing Froude number.

The Reynolds number describes the degree of turbulence achieved in the tank. The effect of the Reynolds number on the mixing time in the tanks is discussed qualitatively by Dickey and Fenic (1976). At low Reynolds number, viscosity has a significant influence on the flow field in the tank, and flow is laminar. Mixing time in agitated vessels is found to vary inversely with the rate of agitator rotation so the product of mixing time and rate of rotation is a constant in the laminar region. As the Reynolds number increases, the flow becomes turbulent, and mixing times diminish more rapidly. When flow is fully turbulent, mixing time is directly proportional to the rate of rotation of the agitator, but the proportionality constant is much smaller than that in the laminar region. This decrease in proportionality constant leads to much smaller mixing times in the turbulent region and should lead to more efficient mixing.

The effect of liquid depth on mixing patterns in propeller stirred vessels was studied by Marr and Johnson (1963). For an impeller centered in the tank, the aspect ratio of the tank was found to have a distinct effect on the flow pattern in the tank and hence mixing. Shallow tanks were found to exhibit a downward flow below the propellers and a recirculating upward flow near the tank walls. Tall tanks exhibited two recirculating zones, one in the lower and one in the upper portion of the tank. The aspect ratio at which the recirculating region first occurs appears to be affected by the ratio of the propeller to tank diameter.

The qualitative change in fluid circulation pattern observed by Marr and Johnson (1963) is significant and suggests that tank geometry can have an important influence on flow pattern. Consequently, geometric similarity appears to be important when performing scaled mixing experiments in tanks. Thus Froude number, Reynolds number, and tank geometry all appear to affect mixing behavior.

### 3.1.2 Jet Mixing of Liquid/Liquid and Single-Phase Fluids

Studies of fluid mixing using jet mixing pumps have been performed by Fox and Gex (1956) and Fosset and Prosser (1951). The time required to mix a constant density fluid injected with a jet mixer was studied by Fox and Gex (1956). The specific jet mixer design was not described. Tests were performed using 0.30-m (1-ft) and 1.5-m (5-ft) diameter tanks; one case was performed using a 4.3-m (14-ft) diameter tank. Jet Reynolds numbers ranged between 200 and 100,000. The dimensionless mixing time was influenced by jet Reynolds number; at a jet Reynolds number less than 2000, flow was laminar and could be represented by one relationship; at jet Reynolds number greater than 2000 flow was turbulent and obeyed a different relationship. Froude number affected mixing time in both laminar and turbulent flow regimes.

The results obtained by Fox and Gex (1956) are qualitatively similar to the results found for mixing using mechanical agitators. In both, the Reynolds number is seen to have an important influence at low Reynolds number; the effect is small but non-negligible at higher Reynolds numbers. Also dimensionless mixing time for neutrally buoyant fluids was found to increase with an increasing Froude number.

Jet mixing in large tanks was studied by Fosset and Prosser (1951). Measurements were performed using 25 different tanks with diameters between 4.6 m (15 ft) and 44 m (144 ft). Tank heights ranged from 4.6 m (15 ft) to 11 m (35 ft). An aqueous solution of sodium carbonate ( $\text{NaCO}_3$ ) with a density greater than that of water was injected into the tank. The time required to mix a high density fluid introduced into the tank using the jet mixer was determined by measuring the electrical conductivity of the solution in the tank. The major finding of this study showed that mixing behavior was strongly influenced by gravitational factors, and that densimetric Froude number was the most important parameter affecting dimensionless mixing times. In a second study designed to investigate the effect of densimetric Froude number on jet motion, data show that at low densimetric Froude numbers, the jet was unable to rise to the top of the tank and the fluid in the tank stratified.

A preliminary experiment to mix tank waste was performed in double-shell tank 241-AP-102. In this experiment, limestone was added to a solution of sodium hydroxide in water and used as a slurry simulant. The bulk solids loading that would have been achieved in this experiment if all solids had been suspended was 1.2 Wt%. Analysis indicated that approximately 10% of these solids were suspended in the tank during operation; thus on the average, the slurry contained approximately 0.1 Wt% solids. None of the reported solids measurements exceeded 0.2 Wt% solids. Based on these measurements it is estimated that the jet density never exceeded the fluid density by more than 0.2 Wt% solids during this test. Because uniform mixing appears to have been achieved away from the settled limestone bed, it is likely that the jet was neutrally buoyant; therefore, the jet would be expected to travel to the top of the tank. This was visually observed during the test. Thus test results from tank 241-AP-102 do not contradict the findings of Fosset and Prosser because the solids concentration in tank 214-AP-102 was not large enough to affect the mean jet density.

### 3.1.3 Summary of Factors Affecting Mixing

Dimensionless mixing time in liquid/liquid and single-phase fluids is found to be affected by the Reynolds number, Froude number, and by the aspect ratios describing the tank geometry. The dimensionless parameters found to affect mixing using either jet mixers or mechanical agitators were similar to one another. However, when jet mixers were used, transition to turbulence occurred at a lower Reynolds number. All dimensionless parameters that affect mixing of single-phase fluids were expected to affect solids suspensions in solid/liquid mixing.

## 3.2 SYSTEM DEFINITION

The HWVP feed preparation tank agitation system definition is contained in two reports.<sup>(a),(b)</sup> Information used in conducting the present work was

---

(a) WHC. 1991. Functional Design Criteria, Multi-Tank Waste Storage Facility, Project W-236. W236FDC, Westinghouse Hanford Company, Richland, Washington, October.

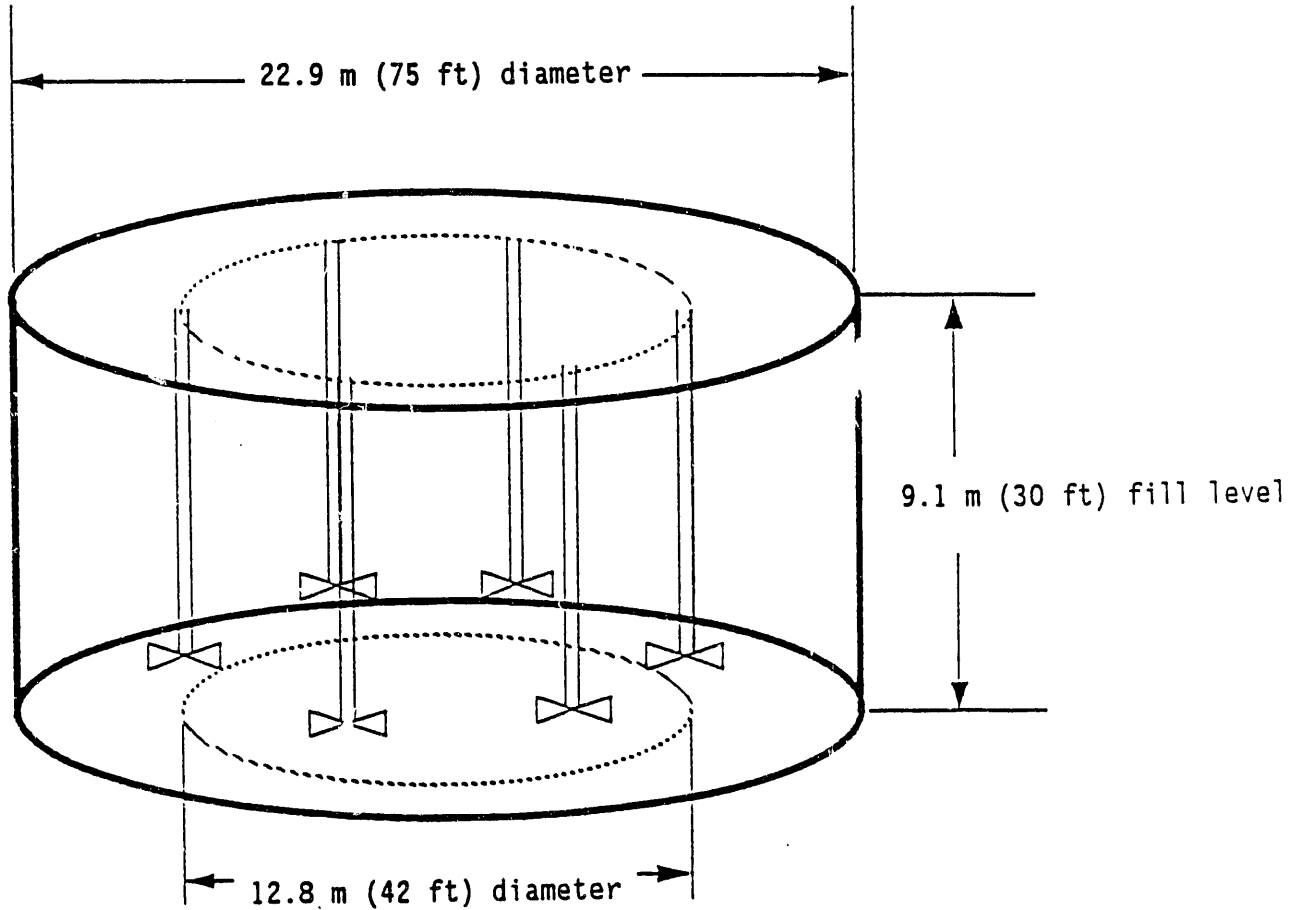


**FIGURE 3.1** Schematic of the Six-Pump Agitation System Proposed for the HWVP Feed Preparation Tanks

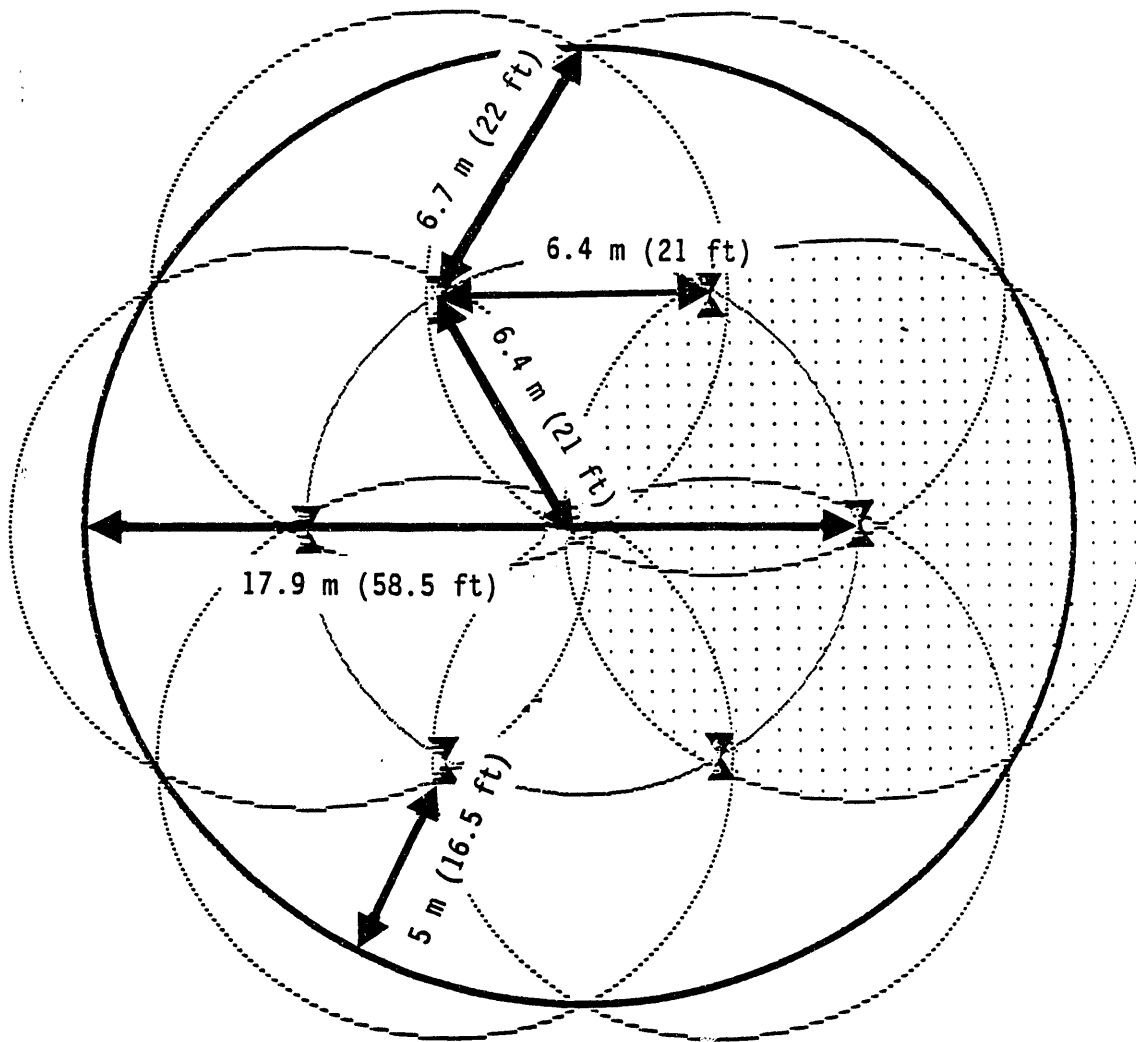
obtained from the first of these, from WHC HWVP project personnel, and from WHC Retrieval Technology project personnel.

### 3.2.1 Geometry

The geometry of the HWVP feed prep tanks and agitation system is presented schematically in Figure 3.1. Six 300-hp mixing pumps are to be symmetrically located on a 6.4 m (21 ft) radius in a 22.9-m (75-ft) diameter

---

(b) KEH. 1991. Preliminary Conceptual Study, Multi-Tank Waste Storage Facility, Project W-236. WHC-SD-W236-PCS-001, Rev. 0, Kaiser Engineers Hanford Company, Richland, Washington, August.



22.9 m (75 ft) tank diameter

Six dual jet mixer pumps on 6.4 m (21 ft) radius

**FIGURE 3.2** Planar View Schematic of Pump Locations

tank. Each tank is to have a 3% grade sloped floor with the low point at the center. A planar view schematic of the pump locations and geometric parameters such as linear distance to adjacent pumps is shown in Figure 3.2. When on a 6.4 m (21 ft) radius, the distance to an adjacent pump is 6.4 m (21 ft). The nearest distance from the pump centerline to the tank wall is 5.0 m (16.5 ft). The maximum distance to a wall that a jet would have to traverse

(assuming all six pumps are operating) is 6.7 m (22 ft). The maximum distance to any wall is 17.9 m (58.5 ft).

### 3.2.2 Pump Description and Operating Conditions

A schematic of a mixing pump is presented in Figure 3.3. Each pump has a bottom intake and two 0.15-m (0.5-ft) diameter jet nozzles directed in opposite directions. The six pumps are to be hung on shafts suspended from the tank dome and each of the pumps is to oscillate through a prescribed angle. Pump parameters of particular concern to the present work are listed in Table 3.1.

TABLE 3.1 Pump Design Parameters

<u>Design Parameters</u>	
Pump rotation rate	0.1 rpm
Pump rotation angle	180. degrees
Pump nozzle diameter, $D_0$	0.15 m (0.5 ft)
Pump nozzle discharge velocity, $U_0$	17.9 m/s (58.8 ft/s)
Nozzle discharge parameter, $U_0 D_0$	2.73 m <sup>2</sup> /s (29.4 ft <sup>2</sup> /s)

It was neither an objective of the present work nor part of the scope of work to consider pump turndown or to analyze heating effects of long-term operation of the pumps.

### 3.3 DOUBLE-SHELL TANK WASTE PHYSICAL PROPERTIES

The HWVP feed preparation tanks and agitation system are expected to be subjected to a variety of high-level liquid radioactive wastes as wastes in double-shell tanks (DSTs) on the Hanford site are retrieved.

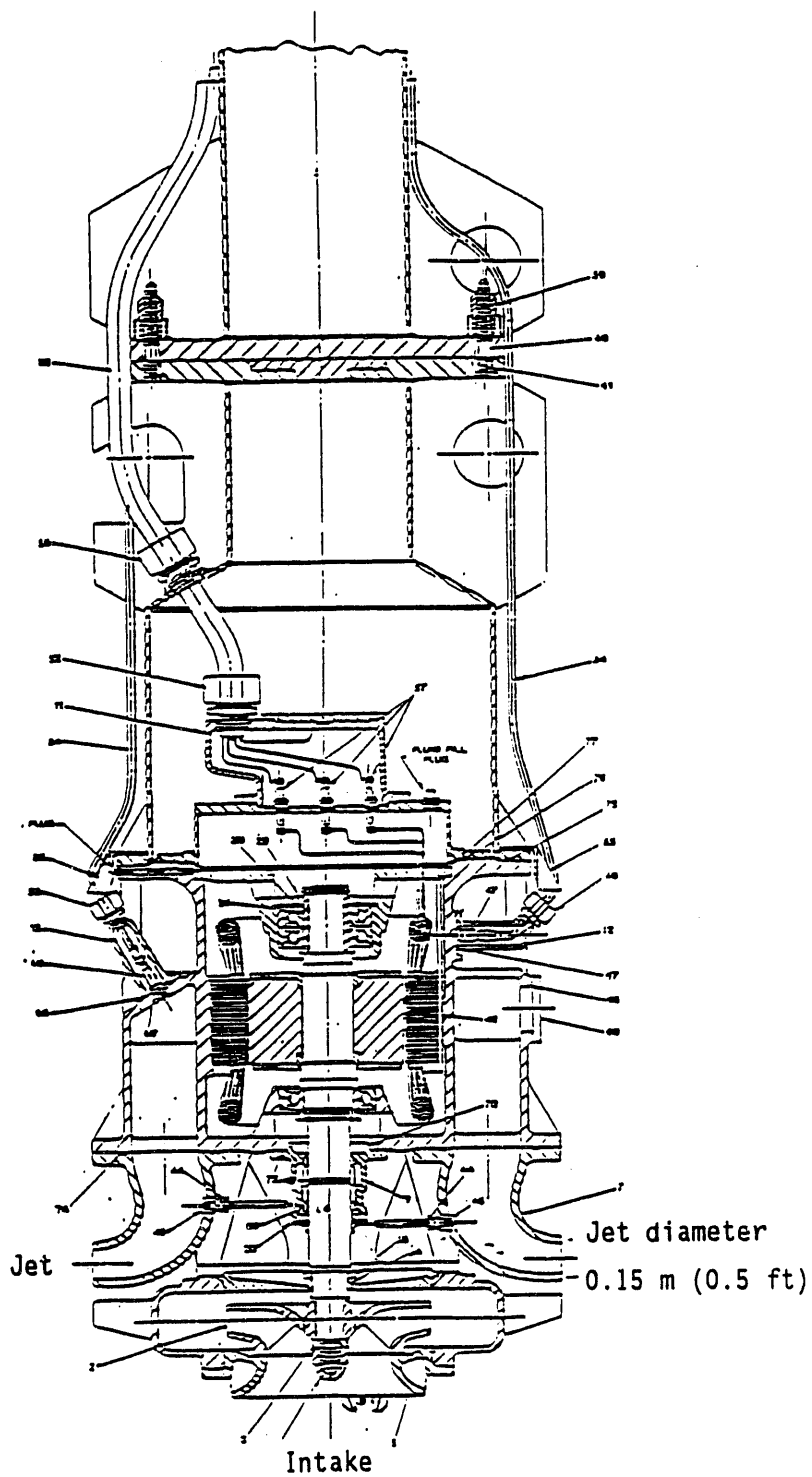


**FIGURE 3.3** Schematic of a Mixing Pump Expected to be Similar to Those Planned for HWVP Feed Preparation Tank Agitation

**TABLE 3.2 Upper Limits of Physical Properties Used in Analysis**

<u>Property</u>	<u>Value</u>	<u>Observation</u>
Particle diameter, $d_p$	70 $\mu\text{m}$	high end of range; expect 95% < 50 $\mu\text{m}$
Particle density, $\rho_s$	3 $\text{g/cm}^3$	affects settling rates; coupled buoyancy effects
Fluid density, $\rho_f$	1.05 $\text{g/cm}^3$	mostly water-like liquid; may range up to 1.08 or 1.1 $\text{g/cm}^3$
Viscosity, $\mu_f$	1.00 cP	determined from 1.05 $\text{g/cm}^3$ density sodium nitrate solution in water
Solids concentration	13 Wt%	maximum fully mixed; solids basis; 25 Wt% would probably be an upper limit

Some characterization studies of the liquid and solid materials stored in DSTs have been completed (Peterson, Scheele, and Tingey 1989).<sup>(a),(b)</sup> Based on these analyses and projections of physical and rheological properties anticipated during pretreatment, primary parameters established as upper limits for conducting the present work were defined. See Table 3.2.

The 70- $\mu\text{m}$  particle diameter is to be considered as representative of the upper limit. From characterization data, it is expected that more than 95% of the solids will be less than 50  $\mu\text{m}$ . The particle density of 3  $\text{g/cm}^3$  is a representative number. Most of the particulate material is expected to be somewhat lighter than this, but individual species may exhibit a range of densities. There may be a small fraction of materials with higher particle densities such as heavy metals (Pu) or noble metals (Rh, Ro, Pd). The fluid

---

(a) R. D. Scheele and D. McCarthy. May 1986. "Characterization of Actual Zirflex Decladding Sludge" 105-AW, NCRW. A letter report prepared for Rockwell Hanford Operations. Pacific Northwest Laboratory, Richland, Washington.

(b) J. M. Tingey, R. D. Scheele, M. E. Peterson, and M. R. Elmore. September 1990. "Physical and Rheological Characterization of Waste from Double Shell Tank 103AW". Prepared for Westinghouse Hanford Company by Pacific Northwest Laboratory, Richland, Washington.

in the tank will be a water-based fluid such as a sodium nitrate solution in water. The fluid base viscosity was modeled as that of sodium nitrate solution in water, which is similar to that of water (CRC 1975). The total solids concentration is taken to be 13 Wt% on a solids basis as a specification for the present work. The upper limit on solids would probably be 25 Wt%.

### 3.4 MIXING PUMP CHARACTERISTICS

Mixing pump operation can be separated into two functions: mobilizing the settled solids and/or sludge layer at the tank bottom and maintaining the solids in a suspension of uniform concentration until the slurry is removed from the tank. A discussion of each operation follows.

#### 3.4.1 Mobilizing Settled Solids

Two mechanisms for sludge mobilization have been described by Powell.<sup>(a)</sup> Jets may mobilize solids by erosion caused by shearing action of a high velocity fluid moving parallel to the surface of a sludge bank or by bulk mobilization of sludge caused by impact of a high velocity jet normal to the sludge bank. The mechanism that will dominate during a particular physical situation will depend upon a number of factors including the velocity of the fluid near the sludge bank, the shape of the sludge bank, the size of particles in the sludge, and inter-particle forces between solids in the sludge. Erosion may be important during some stages of mobilization while bulk mobilization may be important during others.

Powell proposed that the shear strength of the sludge described the ability of the sludge to resist mobilization. Correlations proposed by Powell to describe mobilization by erosion and bulk mobilization agree with a more general relationship between the maximum diameter circle cleaned [effective

---

(a) M. R. Powell, C. L. Fow, G. A. Whyatt, P. A. Scott, and C. M. Ruecker. November 1990. Proposed Test Strategy for the Evaluation of Double-Shell Tank Sludge Mobilization. A letter report for Westinghouse Hanford Company by Pacific Northwest Laboratory, Richland, Washington.

cleaning radius (ECR)] and jet nozzle diameter ( $D_0$ ) as a function of the Reynolds number (Re) and a yield parameter ( $N_T$ )<sup>(a)</sup>

$$ECR/D_0 = f(Re, N_T) \quad (3.1)$$

$$N_T = (\rho_f U_0^2)/\tau_{ss} \quad (3.2)$$

$$Re = (\rho_f U_0 D_0)/\mu_f \quad (3.3)$$

where  $\rho_f$  is the fluid density,  $U_0$  is the jet nozzle exit velocity,  $\tau_{ss}$  is the shear strength of the sludge, and  $\mu_f$  is the fluid viscosity.

Experiments to determine the effective cleaning radius using scaled mixing pumps were analyzed by Powell. Yield parameter was matched in these experiments. Results fell into groups based on simulant type. For clay/water and soda ash simulants, effective cleaning radius was found to be a function of shear strength. However, this relationship did not predict effective cleaning radius for polymer simulant such as kaolin/Ludox. These investigations are continuing. Powell has recently suggested that tensile strength may be a more useful parameter to characterize sludge resistance.

#### 3.4.2 Maintaining Solids in Suspension

Two basic mechanisms are important during solids suspension: 1) large-scale circulation flow patterns and 2) small-scale diffusive motion. Mixing is expected to occur as a result of large-scale circulation patterns induced by mixing pump jets. Particles may be transported to the upper regions of a tank by a coherent jet provided that 1) the jet is particle laden and 2) the jet is capable of traveling to the upper portions of the tank. Eventually as the distance from the nozzle increases, the jet loses momentum and particles are expected to fall by gravity to lower regions of the tank.

Large-scale circulation patterns could be seriously affected by slight density differences in the tank. The average density of the jet is affected

---

(a) L. M. Liljegren. May 1992. Similarity Analysis Applied to the Design of Scaled Tests of Hydraulic Mitigation Methods for 214-SY-101, Draft. Pacific Northwest Laboratory, Richland, Washington.

by its particle loading. The jet intake is located at the bottom of the tank; therefore, the jet density may be greater than the density of the surrounding fluid; this excess density relative to the surrounding fluid will increase as the jet rises to the upper regions of the tank where particle loading is lower. Excess density, combined with low momentum, can have a dominant influence on the jet motion. When a dense jet emits upward, gravity tends to retard the jet. The jet will only reach the upper regions of the tank if its momentum is sufficiently large to overcome the force of gravity. The height to which a jet will rise ( $H_j$ ) is a function of the densimetric Froude number based on jet diameter ( $Fr$ ), the relative density difference between the jet and the surrounding fluid ( $N_{\rho_j}$ ), the jet angle with respect to the floor ( $\theta$ ), and the jet Reynolds number ( $Re$ ).

$$H_j/D_0 = f(Fr, N_{\rho_j}, \theta, Re) \quad (3.4)$$

$$Fr = U_0 / (N_{\rho_j} g D_0)^{1/2} \quad (3.5)$$

$$N_{\rho_j} = \Delta\rho / \rho_j \quad (3.6)$$

where  $g$  is gravitational acceleration,  $\Delta\rho$  is the density difference between the jet and the surrounding fluid, and  $\rho_j$  is the jet density as it exits the nozzle. When the relative density difference of the jet is large, the Froude number is low and the jet will be strongly influenced by gravity. For jet mixing, both the density of the jet at the nozzle and the density difference between the jet and the surrounding fluid will depend upon the degree of mixing achieved.

Experiments are planned as a part of double-shell tank retrieval investigations at PNL to investigate the effects of Reynolds number, Froude number, and gravitational settling parameter (Bamberger, Liljegren, and Lowery 1993; Liljegren and Bamberger 1992). Gravitational settling parameter is an equivalent method to account for the relative density difference shown in Equation (3.6). These experiments will be used to validate computational code performance.

#### 4.0 COMPUTER MODELING OF FEED TANK AGITATION SYSTEM

Computations were conducted using the TEMPEST<sup>(a)(b)</sup> computer program. A modeling approach using a single, centrally-located, rotationally-oscillating mixing pump with two dual-opposed jets was used consistent with modeling analysis conducted for the DST Retrieval Project. Calculations were conducted for the prescribed tank design and tank contents, as described in Section 3. Calculations were conducted for particulate of two diameters (10  $\mu\text{m}$  and 70  $\mu\text{m}$ ) in a supernatant. Cases of three fluid depths [9.1, 5.3, and 2.2 m (30, 17.3, and 7.6 ft)] were computed. Results analyzed were 1) the hydrodynamics of the mixing jets in the tank including the development of the free jet into a floor jet, 2) the ability of the jets to "climb" the tank wall and induce circulation throughout the liquid volume, and 3) the level of turbulent shear stress generated by the mixing jets on the tank floor. These are the dominant mechanisms affecting the ability of the mixing pump and jet design to maintain material uniformly mixed in the liquid volume and to prevent excessive amounts of material from building up on the tank floor.

#### 4.1 OBJECTIVES OF COMPUTER MODELING

The objectives of the computer modeling are to analyze the hydrodynamics of the mixing of turbulent jets in the HWVP feed preparation tanks and to determine the propensity to maintain particulate material uniformly distributed throughout the tank volume.

#### 4.2 BACKGROUND

Computer modeling of jet mixing in waste storage tanks is being conducted within several programs at PNL to support waste remediation and retrieval on the Hanford site. These include the Double-Shell Tank Retrieval Project, the Waste Tank Safety Program (Tank 101-SY Mitigation), and Pretreatment Technology. Each of these programs has special analysis needs;

---

(a) Transient, Energy, Momentum, and Pressure Equation Solution in Three-dimensions.

(b) The code documentation is described in Trent and Eyler (1992).

computer modeling of the fluid dynamics of mixing and solid/liquid transport is inherent to each. The modeling in progress at Pacific Northwest Laboratory uses the TEMPEST computer program (Trent and Eyster 1992).

TEMPEST is a three-dimensional, time-dependent, computational fluid dynamics analysis computer program that solves discretized equations for the conservation of mass, momentum, thermal energy, turbulence, and species transport. The code is well suited to model the turbulent, jet-induced mixing in waste storage tanks.

#### 4.3 MODELING APPROACH

The modeling approach used for this analysis is based on a sequence of calculations developed during the DST Retrieval Project to prepare pre-test predictions of scaled experiments to model concentration distribution during forced mixing by mixer pump.

##### 4.3.1 Analysis Steps

The analysis steps used in the computations are as follows. Once a given set of parameters are defined for a simulation, a fully coupled hydrodynamic calculation is conducted over several pump oscillation cycles. This is done without including a particulate (species) phase. The particulate phase is then included in a restart calculation over one cycle. Confirmation of solution of the transport of the species phase is done by assuming that the species phase is of the same density as the supernatant. Later, the species phase representing the more dense particulate material is implemented and a calculation conducted over one cycle of time. Hydrodynamic results are then compared to ascertain the effect of coupling between the continuous phase (liquid) and the distributed phase (solids) through buoyancy and concentration-dependent viscosity.

During one of these cycles, flow and turbulence variable fields are routed to a file at regular intervals. These fields are then processed into a recycle file. To compute longer-time simulation of the species transport, the recycle file is used repetitively in lieu of computing the complete, fully-coupled hydrodynamics, which provides a computational gain of nearly 140 times. This computational gain is significant to the analysis because at jet

velocities on the order of 18 m/s (60 ft/s), approximately 100 CPU hours of time are needed on an IBM 530 superworkstation (this machine is approximately 0.32 of Cray XMP speed) to compute each pump oscillation cycle in the fully-coupled hydrodynamic mode. The use of the recycle file approach is valid as long as there is little or no coupling between the phases through buoyancy or concentration-dependent viscosity.

Results from the computations are analyzed by post-processing techniques using data stored on computer files during the computations. Data files generated during this work amounted to nearly 1 gigabyte of file storage.

#### 4.3.2 Assumptions

Assumptions (both inherent and explicit) are required for any computational analysis approach that solves conservation transport equations in fluid dynamics. There are inherent assumptions built into the discretization of the equations (such as grid resolution and numerical diffusion), explicit assumptions built into models of physical processes (such as phase interactions between dispersed solids, liquids, and solid walls), and modeling assumptions concerning boundary conditions, etc. It is not the objective of this work to exhaustively address the significance of each of these. But it is important to point out certain assumptions that have primary significance to the present problem.

The computational domain limitation of the coordinate system used by TEMPEST coupled to the modeling approach for a rotationally-oscillatory mixing pump with dual-opposed turbulent jets has only been proven for use in a centrally-located pump situation in cylindrical coordinates. Thus, it is assumed that significantly important information can be obtained from such a model as to be pertinent to analysis of the six-pump design. Furthermore, it is necessary to model the floor as flat in situations where a pump model rotates. Thus, it is assumed that the flat-floor model of the tanks is applicable. This assumption is investigated separately by analyzing the effect of a sloped floor using a nonrotating pump model.

In the TEMPEST modeling approach, coupling between the solid and liquid phases occurs through buoyancy and concentration-dependent viscosity as the heavier solid phase settles with time. It is explicitly assumed in the

TEMPEST model that a solid phase consists of small, inertialess particles. This assumption is valid as long as particles in the tank are less than about 200  $\mu\text{m}$  in size. It is furthermore assumed that the solids phase can be represented as a continuum of well-separated, discrete particles and that high concentrations of settled material remains shearable according to a Newtonian relation.<sup>(a)</sup>

At the floor of the tank, particle deposition and erosion are modeled through a local equilibrium interchange approach. This model approach assumes that 1) the layer of material that builds up during operation is thin relative to the computational grid resolution along the floor of the tank, 2) there is no bed load transfer, and 3) there could be hysteresis in deposition and erosion. In this analysis it is conservatively assumed that there is no hysteresis effect in the erosion and deposition.

#### 4.3.3 Settling Velocity

Particle settling velocities ( $V_s$ ) used in the analyses were determined from the Stokes settling relation

$$V_s = (2/9) (d_p/2)^2 g (\rho_s - \rho_f) / \mu_f \quad (4.1)$$

where  $d_p$  is the particle diameter,  $g$  is gravitational acceleration,  $\rho_s$  is solids density,  $\rho_f$  is fluid density, and  $\mu_f$  is fluid viscosity. Equation (4.1) is valid for particle Reynolds number ( $Re_p$ )

$$Re_p = (\rho_f d_p V_s) / \mu_f < 1 \quad (4.2)$$

Table 4.1 lists the settling velocity and particle Reynolds number for the parameters of this problem.

---

(a) Very recent TEMPEST investigations have implemented a non-Newtonian model of a Bingham plastic fluid with yield to better model certain physical aspects of sludges. This model was not available to conduct the present work.

**TABLE 4.1 Particle Settling Velocity Calculation**

		<u>Parameter</u>	<u>Value</u>		
		Fluid density, $\rho_f$	1.05 g/cm <sup>3</sup>		
		Fluid viscosity, $\mu_f$	1.00 cP		
Particle Size, $\mu\text{m}$	Particle Specific Gravity	Particle Settling Velocity		Reynolds Number, $Re_p$	Unhindered Settling Time to 9.1 m (30 ft), min
		m/s	ft/min		
10	1.60	$2.79 \times 10^{-4}$	0.055	0.0001	545
70	3.00	$4.93 \times 10^{-3}$	0.97	0.34	31

Note that the settling velocity for the 70  $\mu\text{m}$  particles with a specific gravity of 3.0 is quite large. At this settling rate, approximately 1/3 of the material would reach the floor in the time a pump makes a complete oscillation cycle at a rotation rate of 0.1 rpm.

#### 4.3.4 Single-Pump, Dual-Jet, Flat-Floor Model

A schematic of the computational domain used for analysis of mixing in the tank is presented in Figure 4.1. A computer model consisting of a 180 degree section of the tank was used with a single, centrally-located mixing pump. The mixing pump has two jets. Thus the half-tank-model approach is valid using periodic boundary conditions along the center plane. A total of 7942 computational cells were included in the computations. The numbers (1 through 16) in Figure 4.1 represent locations where time-history information was monitored during computations.

#### 4.3.5 Resuspension Deposition Model

Particulate resuspension and deposition on the floor of the tank were modeled using a critical shear stress floor model. This model links with the conservation-of-particle-species suspension model coded into TEMPEST at the floor boundary condition by modeling the net sediment flux at the floor as a function of local flow conditions and local solid phase mass fraction. It is well understood that the deposition/resuspension process exhibits hysteresis when considering the net flux of the solid phase at the bed boundary.

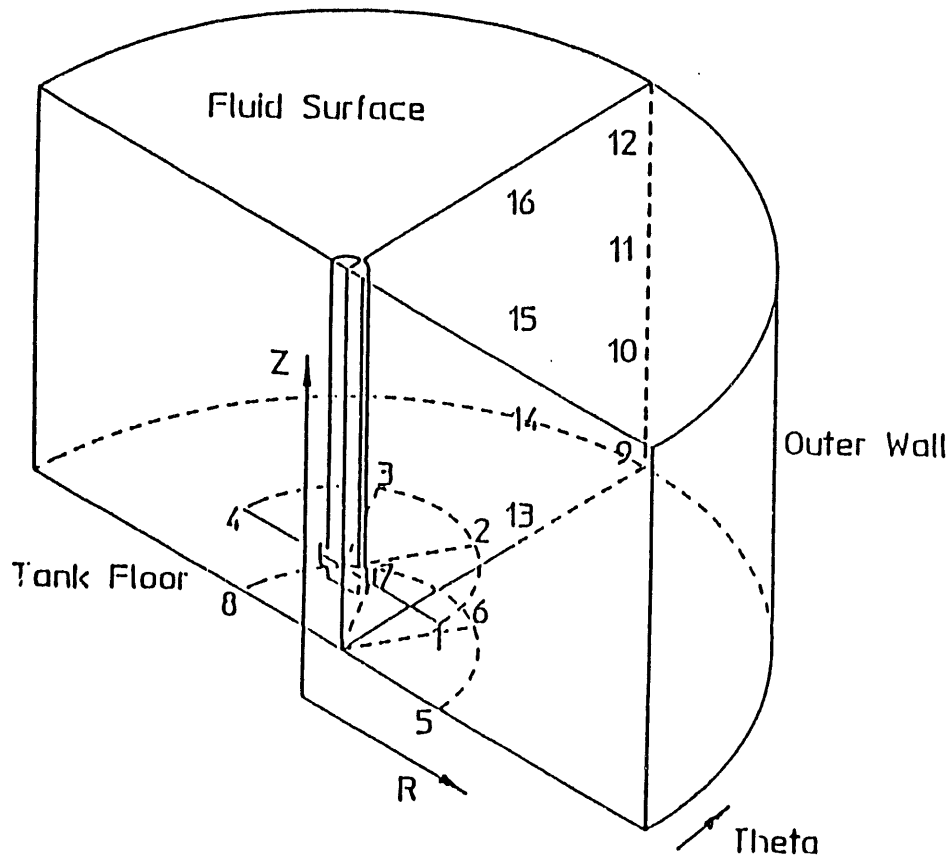


**FIGURE 4.1** Schematic of the Computational Domain of the Flat-Floor Model with a Single, Centrally Located Mixing Pump with Two Jets. Numbers correspond to time dependent monitor curve locations.

That is, the threshold stress at which net resuspension begins is generally higher than the threshold stress at which net deposition ends. This situation allows for some finite stress range at which the net sediment flux is zero and the bed is in equilibrium with the suspension. This commonly observed physical behavior is expressed most simply by the semiempirical relations:

For  $\tau < \tau_d$  (material being deposited)

$$m = \rho_m V_s \Phi (1 - \tau/\tau_d) \quad (4.3)$$

For  $\tau > \tau_r$  (material being resuspended)

$$m = R(1 - \tau/\tau_r) \quad (4.4)$$

For  $\tau_d < \tau < \tau_r$  (no material interchange between the bed and fluid)

$$m = 0 \quad (4.5)$$

In the above expressions,  $m$  is the species mass flux,  $\rho_m$  is the mixture density,  $V_s$  is the particle settling velocity,  $\phi$  is the species mass fraction,  $\tau$  is the fluid shear stress at the fluid/bed boundary,  $\tau_d$  is the critical shear stress for deposition,  $\tau_r$  is the critical shear stress for resuspension, and  $R$  is the resuspendability of the sediment species.  $\tau_d$ ,  $\tau_r$ , and  $R$  are empirical constants. Bed shear stress ( $\tau$ ) is computed during the computational analysis. The species mass flux ( $m$ ) is thus a boundary source term to the species particle suspension transport equation at the interface between the bed layer and the transporting fluid.

The Equations (4.3) to (4.5) are a commonly used model for calculating the sedimentation of fine particles (Onishi, Dummuller and Trent 1989, Onishi and Trent 1985, 1982). Equation (4.4) for resuspension is similar to the expression in use in the DST Mobilization Task.<sup>(a)</sup> It is generally accepted that for meaningful particle resuspension to occur, the boundary layer at the sediment bed must be turbulent because turbulent bursting is the primary mechanism for small particle resuspension (Fromentin 1989). Turbulent bursting is a large-scale fluid motion characterized by the periodic eruption of slow moving fluid from the viscous sublayer into the main body of the boundary layer.

Of primary concern in the present application of the erosion-deposition model is determination of the critical shears for resuspension ( $\tau_r$ ) and deposition ( $\tau_d$ ) for the particulate material expected in the HWVP feed

---

(a) M. R. Powell. February 1991. Current Status of DST Sludge Mobilization Research. An Interim Draft Report prepared for Westinghouse Hanford Company by Pacific Northwest Laboratory, Richland, Washington.

preparation tanks. These numbers are not known with a great deal of certainty. The basis for the numbers used in the present work is discussed.

#### 4.3.6 Resuspension Deposition Shear Stress Data

A brief review of sedimentation literature was conducted to determine values of the critical shear stresses for deposition ( $\tau_d$ ), and resuspension ( $\tau_r$ ) and the resuspendability constant (R). A very large range of values may be found in the literature for small particles (small here referring to something less than 100  $\mu\text{m}$ ). Most data are for situations of sand and silt transport in moving surface water (rivers, canals, bays). As an example, Teeter (1988) reports measured critical shear stress of resuspension ( $\tau_r$ ) of 0.599 dyne/cm<sup>2</sup> (0.00125 lbf/ft<sup>2</sup>) and an resuspendability constant (R) of 4.00x10<sup>-7</sup> g/cm<sup>2</sup>-s (8.19x10<sup>-7</sup> lbf/ft<sup>2</sup>-s) for very fine silt (on the order of 1 to 2  $\mu\text{m}$  in diameter). O'Brien et al. (1988) measured a much larger value of  $\tau_r$  [358 dyne/cm<sup>2</sup> (0.747 lbf/ft<sup>2</sup>)] for a lightly packed layer of a larger particulate material with similar size as considered in the present work and quite larger values of resuspendability than Teeter's. Powell<sup>(a)</sup> reports resuspendability constants (R) ranging from 0.015 to 14.7 g/cm<sup>2</sup>-s (0.031 to 30.2 lbf/ft<sup>2</sup>-s) and resuspension critical shear stresses of 0.072 to 2.4 dyne/cm<sup>2</sup> (1.5x10<sup>-4</sup> to 5.0x10<sup>-3</sup> lbf/ft<sup>2</sup>) for various simulated sludges that were obtained by curve fitting data for effective cleaning radius during mobilization in a scaled experiment. Powell is currently refining the understanding of what effects these numbers have in simulant modeling.

Based on this review the parameters listed in Table 4.2 were chosen for the two particle size materials considered.

**TABLE 4.2** Resuspension and Resuspendability Parameters

Particle Size ( $d_p$ )	10 $\mu\text{m}$	70 $\mu\text{m}$
Critical Resuspension Stress ( $\tau_r$ )	11 to 358 dyne/cm <sup>2</sup> (0.023 to 0.747 lbf/ft <sup>2</sup> )	11 to 358 dyne/cm <sup>2</sup> (0.023 to 0.747 lbf/ft <sup>2</sup> )
Resuspendability (R)	1.11 g/cm <sup>2</sup> -s (2.28 lbf/ft <sup>2</sup> -sec)	1.11 g/cm <sup>2</sup> -s (2.28 lbf/ft <sup>2</sup> -sec)

---

(a) M. R. Powell. 1991. Current Status of DST Sludge Mobilization Research. An Interim Draft Report to Westinghouse. Pacific Northwest Laboratory, Richland, Washington. February.

The conservative assumption that the critical deposition shear stress equals the critical resuspension shear stress ( $\tau_d = \tau_r$ ) was made for all calculations in the present work. Furthermore, because of the uncertainty of the character of the material expected in the tanks, the question of applicability of sedimentation data in surface water movement, and variability of such data, it was decided that parameterization was the best way to gain an understanding of the mixing potential of the six-mixer pump design for the HWVP feed preparation tanks.

#### 4.3.7 Effect of Sloped Floor

A slightly modified analysis approach was used to investigate the effect of the sloped floor. To model the effect of the sloped floor, it was necessary to offset the pump model in the tank to a location where the floor sloped. At such an offset location, it is not possible with present modeling capabilities to include the pump rotation because of grid discretization limitations. An effort is currently underway to implement an analytical bipolar coordinate system (Korn and Korn 1968) in TEMPEST. However, assuming that for a single offset pump the two conditions of primary interest are 1) the mixing jet characteristics associated with a jet pointed directly at the nearest wall and 2) a jet pointed directly at the farthest wall, it is sufficient to treat a nonrotating pump with jet axes aligned with a diametral plane. Thus, calculations of the floor-slope effect were conducted in a three-dimensional Cartesian geometry model using a centerplane symmetry. The sloped floor was included in the calculations through the use of a generalized coordinate grid generation tool and the corresponding generalized coordinate solution capabilities of the TEMPEST code.

#### 4.3.8 Extension of Single Pump Modeling to Six-Pump Design Conditions

Results from the single-pump analyses are extrapolated to the six-pump design case by 1) considering the mixing characteristics of both the single, centrally-located, rotationally-oscillatory pump and 2) the single, offset, nonrotating pump cases.

#### 4.4 RESULTS OF SINGLE-PUMP, FLAT-TANK FLOOR MODEL WITH PUMP ROTATION

Results computed for the centrally-located, rotationally-oscillatory, dual-jet, mixing pump computer model are presented and discussed in this section. The computational cases are summarized. The flow-field character of the mixing jet in the tank is presented along with calculated results for the transport of the particle field representing the solids phase. A discussion of the application of these results to the six-pump design basis configuration is presented subsequently.

##### 4.4.1 Computational Cases

Cases computed in the present work for hydrodynamics analyses are listed in Table 4.3. In the table, hydrodynamics-only cases were used to establish flow conditions for the long-time recycle methodology. Uncoupled cases were used during preliminary testing to assure that species settling and distribution were being computed correctly prior to fully coupling. Fully coupled cases include buoyancy effects.

Cases computed with the long-time recycle computational methodology are listed in Table 4.4. In Table 4.4, the X indicates a computation that was completed. In the resuspension-deposition model, there are large discrepancies in critical shear stress reported throughout the sediment literature. For the present work, the effects of this parameter were parameterized. Choosing to set critical shear stress for deposition equal to critical shear stress for resuspension ( $\tau_d = \tau_r$ ) is a conservative assumption made in this work.

##### 4.4.2 Hydrodynamic Results

The characteristic flow field in the tank induced by the mixing jet governs the ability of the design to maintain the material uniformly mixed throughout the tank volume. Upon reaching the tank wall, the ability of the jet to "climb" the outer tank wall is of most importance to transport particulates to the top surface of the liquid. The characteristics of the mixing as it transforms from a turbulent free jet to a floor jet govern the ability to resuspend particulate material that deposits on the tank floor. Calculations were conducted to investigate the pertinent characteristics of the jet hydrodynamics.

**TABLE 4.3 Hydrodynamic Computation Cases**

Fluid Depth		Elapsed Time, min	Number of Cycles	Computational Conditions
m	ft			
9.1	30.0	0 to 40	4	Hydrodynamics only
		20 to 40	2	Uncoupled
		30 to 40	1	Fully coupled
5.3	17.3	0 to 20	2	Hydrodynamics only
		10 to 20	1	Fully coupled
2.3	7.6	0 to 20	2	Hydrodynamics only
		10 to 20	1	Fully coupled

**TABLE 4.4 Solids Transport (Long-Time Recycle) Computational Cases**

Fluid Depth		Particle Size $\mu\text{m}$	Critical Shear Stress $\tau_d = \tau_r$		
m	ft		High	Medium	Low
9.1	30.0	70	X	X	X
		10	X	X	X
5.3	17.3	70	X		
		10			
2.3	7.6	70	X		
		10			

Figure 4.2 presents a comparison of the predicted velocity profiles of the floor jet in a vertical plane through the center of the jet axis for three fluid depths: 9.1, 5.3, and 2.3 m (30, 17.3, and 7.6 ft). With the exception of the location of the fluid-surface boundary, the simulations were conducted identically. Of primary significance in these results is the observation that the floor jet characteristic changes markedly for the lowest fluid depth case. It appears that the presence of the fluid surface has a significant effect in limiting the development of the floor jet by providing a hindrance to entrainment. Furthermore, the lowest fluid depth case has a much greater propensity for the jet flow impinging on the outer tank wall to move tangentially around the tank, rather than "climb" the outer wall.

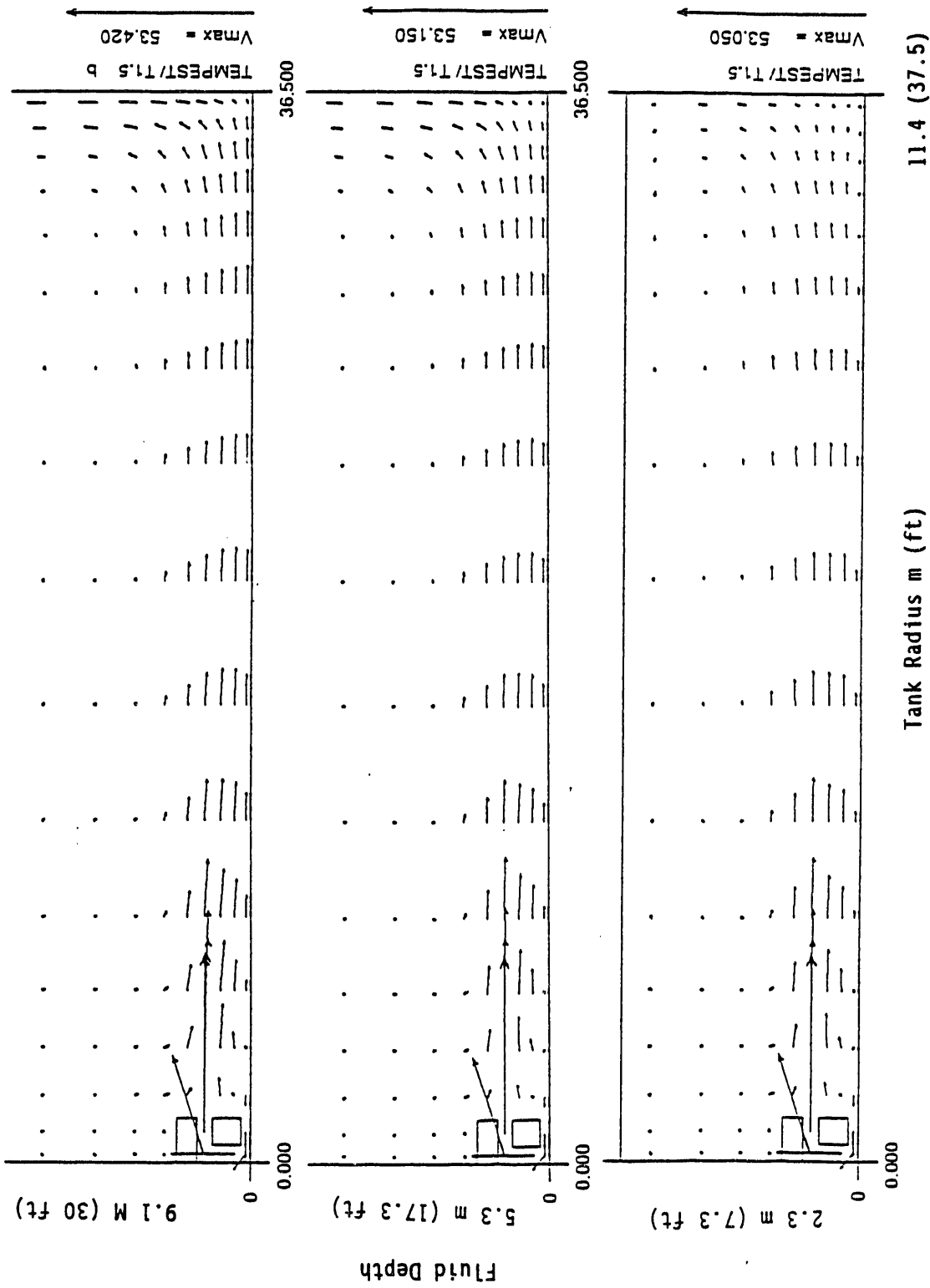


**FIGURE 4.2** Comparison of the Velocity Profiles of a Floor Jet Computed for Fluid Depths of 9.1, 5.3, and 2.3 m (30, 17.3, and 7.6 ft) 11.4 (37.5)

This effect is more clear when the flow fields adjacent to the tank floor are compared for the three fluid depth cases, as presented in Figures 4.3 through 4.5. It is quite apparent that the lowest fluid depth case has considerably more azimuthal flow character than the two deeper fluid cases. This is understandable when one considers that fluid moves in the path of least resistance, and it is easier for the fluid to move laterally than through the free surface, which is modeled as impenetrable. This observation about the computed results raises an interesting question as to whether a real (deformable) fluid surface would greatly alter the character of the flow pattern predicted here. The deformability of the fluid surface also has significance to other considerations such as aerosol generation during mixing operations with low liquid levels and high jet velocities. The dynamic pressure distributions computed adjacent to the free surface boundary condition may be of use in estimating the effect of surface roiling and hence, aerosol generation. However, these considerations were not part of the present scope of work.

Further evidence of the difference in the character of the floor jet for the three fluid depth cases is presented in Figure 4.6. In Figure 4.6 comparison is made of the shear stress distribution at the floor of the tank along the axis of the jet for the three fluid depths; 9.1, 5.3 and 2.3 m (30, 17.3, and 7.6 ft). Also shown in the figure is the empirical correlation of Rajaratnam (1976) as reported by Powell.<sup>(a)</sup> Other calculations of floor jets with TEMPEST<sup>(b),(c)</sup> have exhibited better agreement than that shown in Figure 4.6 with empirical correlations and data for jets of differing velocity

---

(a) M. R. Powell. February 1991. Current Status of DST Sludge Mobilization Research. An Interim Draft Report Westinghouse. Pacific Northwest Laboratory, Richland, Washington.

(b) L. L. Eyler and J. R. Phillips. 1991. "Numerical Modeling Tank Uniformity, Deposition Erosion Floor Model." 1st Qtr FY 92 Progress Report. Double-Shell Tank Retrieval Project, Uniformity Task. Informal report to Westinghouse Hanford Company by Pacific Northwest Laboratory.

(c) J. R. Phillips. June 1992. Personal correspondence from J. R. Phillips to L. L. Eyler of recent of numerical modeling of mobilization within Double-Shell Tank Retrieval Project, Mobilization Task.

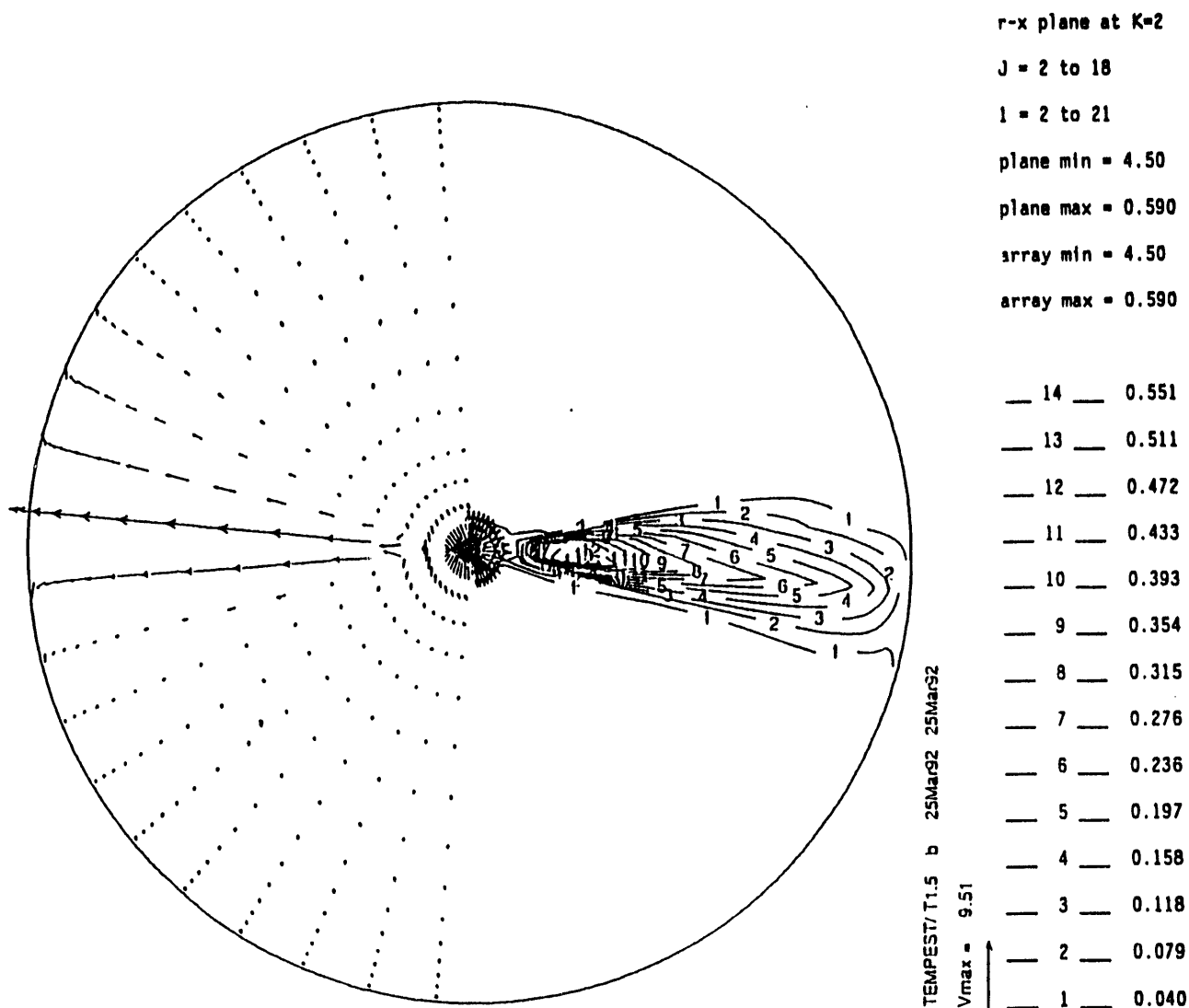


**FIGURE 4.3** Flow Field (Left Half) and Wall Shear Stress Contours (Right Half) at the Floor of the Tank for Fluid Depth of 9.1 m (30 ft)

and at different scale. This is an indication that improvements could perhaps be made to the present predictions. The most likely candidate for improvement would be the use of increased grid resolution.<sup>(a)</sup> However, it is sufficient to note here that all of the shear stress predictions for the three fluid depth cases are conservative. That is, the predicted shear stress is somewhat

(a) D. S. Trent and T. E. Michener. Report of Results of Numerical Modeling of Forced Jet Mixing in Support of Waste Tank Safety - Tank 101SY Mitigation. (In preparation.)

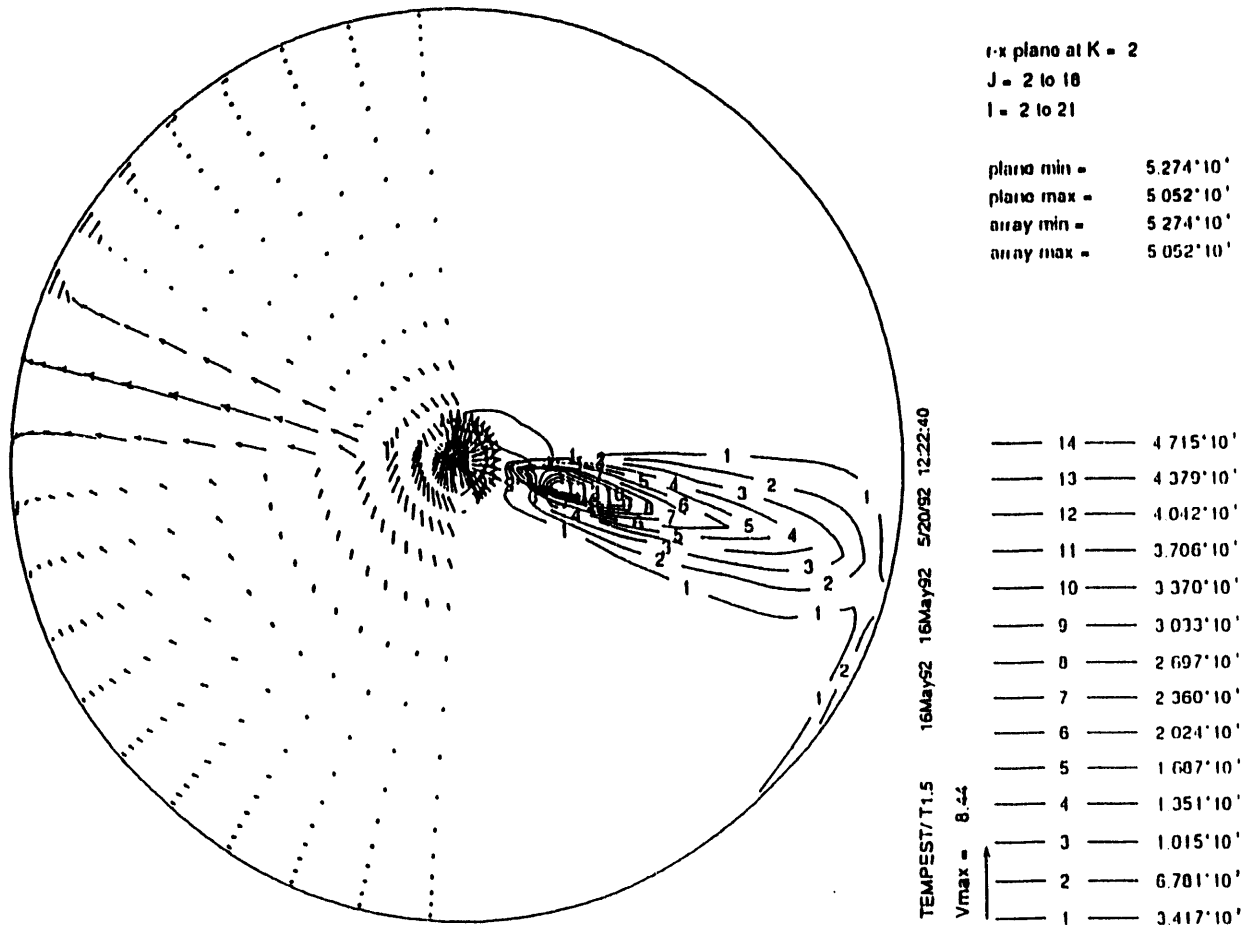


**FIGURE 4.4** Flow Field (Left Half) and Wall Shear Stress Contours (Right Half) at the Floor of the Tank for Fluid Depth of 5.3 m (17.3 ft)

less than expected. Consequently, the amount of deposited material that would be predicted to be eroded and resuspended would be less than would occur in the tanks.

In Figure 4.6, there are several peaks and valleys worth noting. The first peak at the tank centerline ( $R = 0$ ), is caused by the high velocity just under the pump intake. The first valley near  $R = 4$  ft (1.2 m) is the region where there is a stagnation zone. To the left, fluid is moving into the pump intake and to the right, fluid from the jet is moving towards the tank wall.

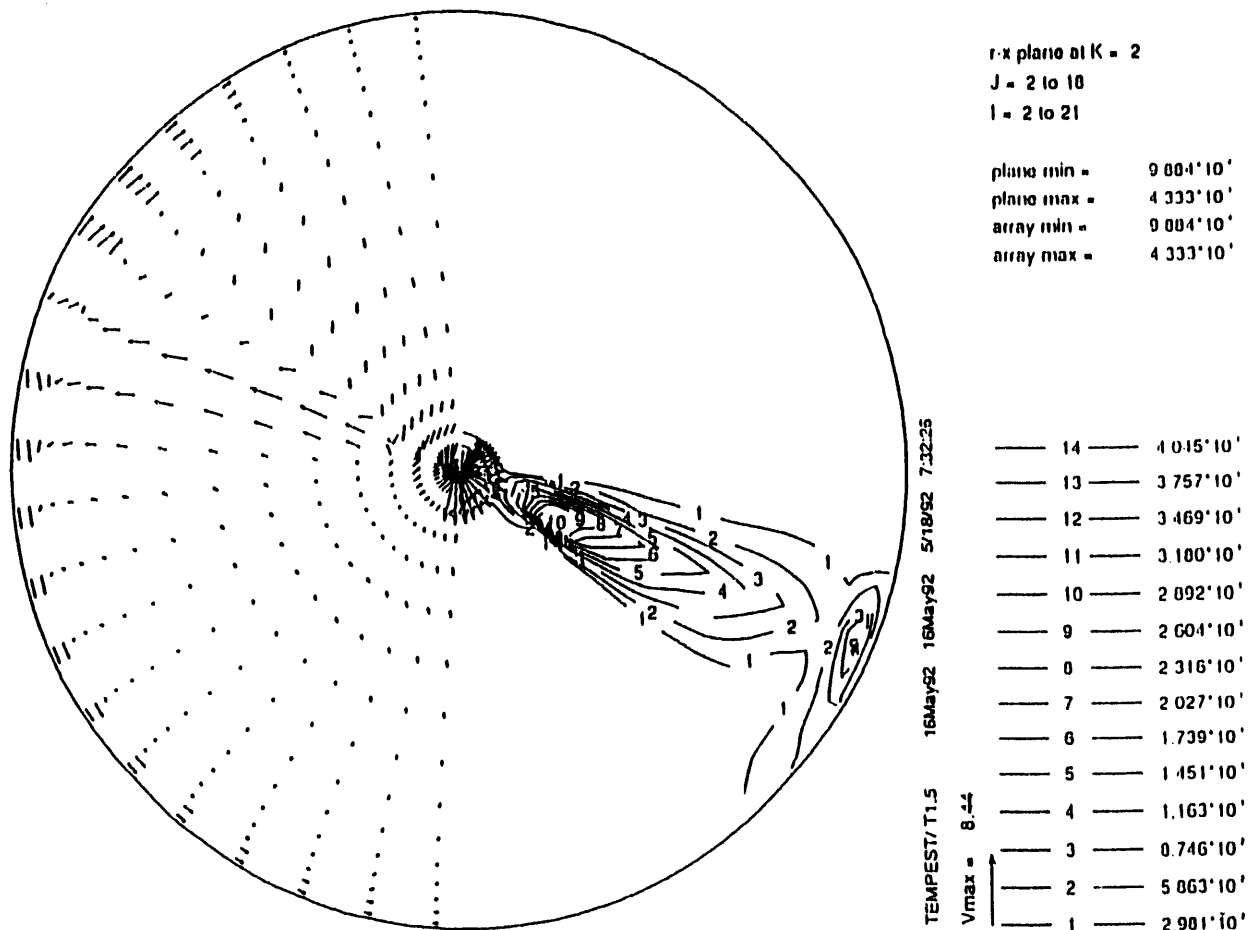


**FIGURE 4.5** Flow Field (Left Half) and Wall Shear Stress Contours (Right Half) at the Floor of the Tank for Fluid Depth of 2.3 m (7.6 ft)

The next peak near  $R = 10$  ft (3.0 m) is the region where the free jet has largely transformed into a floor jet. It is important to note that the shear stress distribution for the lowest fluid depth of 2.3 m (7.6 ft) is nearly a factor of two less than for the other depths. This is interpreted to be a consequence of the fluid surface effect not allowing the full development of the floor jet. Also note that at 11.0 m (36 ft) for the 2.3 m (7.6 ft) fluid depth case, another peak is observed near the outer tank wall. This peak is

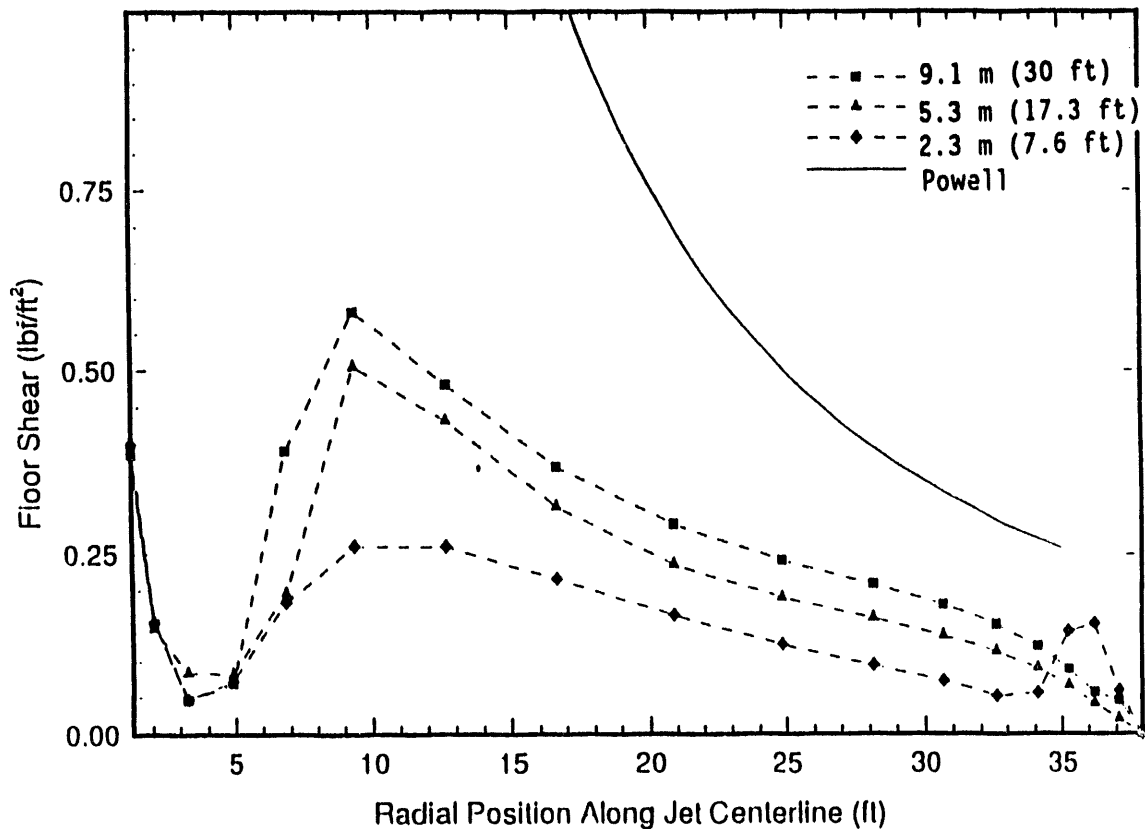


**FIGURE 4.6** Comparison of the Shear Stress Distribution Along the Jet Axis at the Floor of the Tank For Fluid Depths 9.1, 5.3, and 2.3 m (30, 17.3, and 7.6 ft).

caused by the high turbulence shear in the fluid, which is, in turn caused by the character of the jet impinging on the outer wall more as an impinging free jet than as a floor jet because it does not fully attach to the floor.

#### 4.4.3 Solids Transport Results

Several calculation cases were completed for transport of solids in the HWVP feed preparation tank. These were all conducted assuming one, centrally-located, rotationally-oscillatory, dual-opposed mixing pump in a cylindrical tank with a flat bottom. The pump has two jets, equally and oppositely directed. Analysis of results are divided into two primary categories: 1) the material balance of solids that are on the floor as a result of deposition and incomplete resuspension and 2) the distribution of solids throughout the

fluid volume. The former is analyzed through the time-dependence of total material present in the floor layer. The latter is analyzed through the mass fraction distribution as a function of vertical position at fixed points in time.

Figures 4.7 to 4.9 present results of floor density in units of  $\text{lbm/ft}^2$  of material predicted to be deposited into a floor layer. These results are for the same material ( $70 \mu\text{m}$  particles) in a 9.1-m (30-ft) deep fluid for three different critical shear stress assumptions. The first (Figure 4.7) is for the case where the critical shear stress [ $\tau_d = \tau_r = 11 \text{ dyne/cm}^2$  ( $0.023 \text{ lbf/ft}^2$ )] is low relative to the calculated floor shear stresses along the axis of the jet (see Figure 4.6). In this case, all material deposited on the floor between rotational sweeps of the jet is resuspended from the floor layer by the jet. The second case (Figure 4.8) is one for which the critical shear stress [ $\tau_d = \tau_r = 96 \text{ dyne/cm}^2$  ( $0.200 \text{ lbf/ft}^2$ )] is in the range of calculated floor shear stresses along the axis of the jet. The critical shear stress value is between the maximum and the minimum of the jet axis distribution which means that material will be resuspended only over the portion of the jet length where the turbulent shear stress of the jet is greater than the critical value for resuspension. This resuspended material is then redeposited further along the axis of the jet where the local turbulent shear stress of the jet is less than the critical value for deposition. Thus, in Figure 4.8, there is a region where there is little or no material on the floor and a region near the outer tank wall where the material accumulates. The third case (Figure 4.9) is for a critical shear stress that is high relative to any value along the axis of the floor jet. In this case, no material is resuspended by erosion and a relatively flat layer of material accumulates on the floor.

The results in Figures 4.7 through 4.9 are quite informative because they visually show the character of the floor layer depending on whether the critical shear stresses for resuspension and deposition are less than, about equal to, or greater than the turbulent shear stress distribution along the axis of the floor jet. It must be pointed out, however, that the floor density values must be used with caution, especially in Figures 4.8 and 4.9.

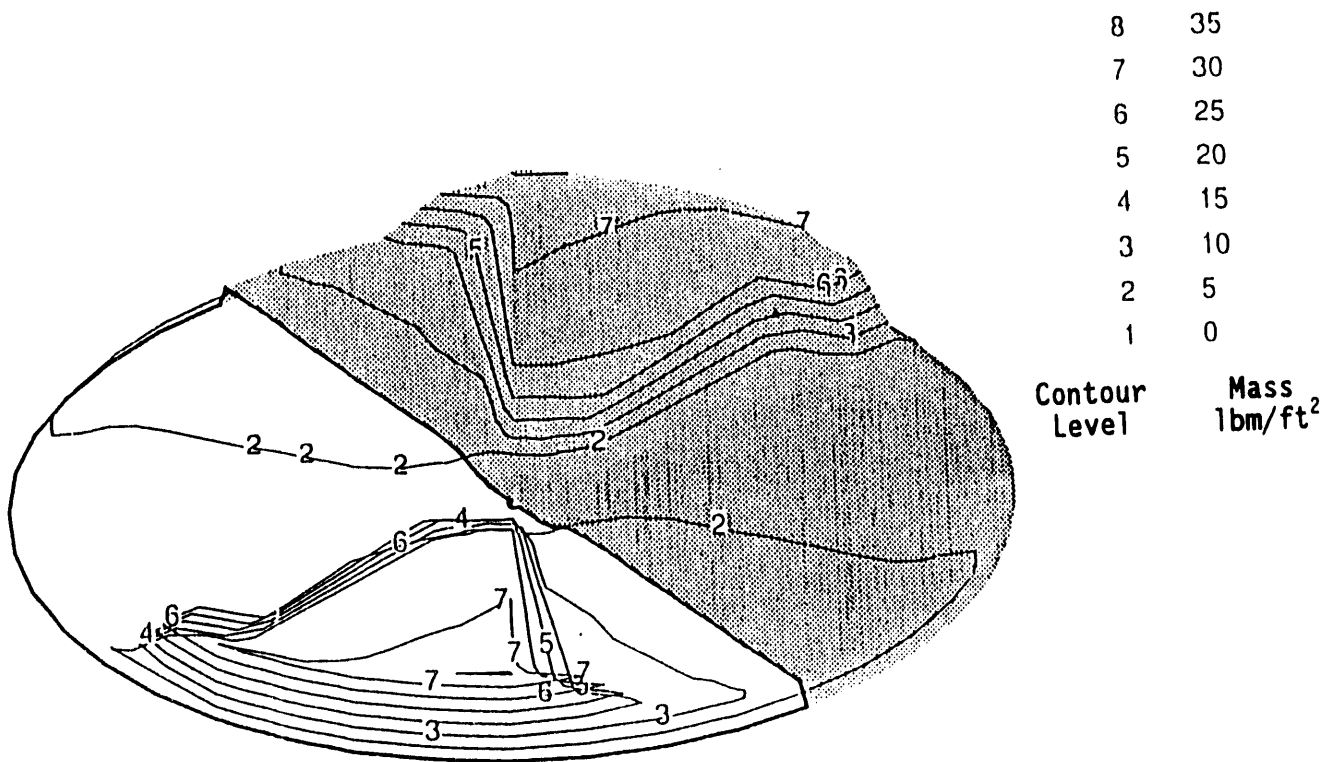


**FIGURE 4.7** Surface Representation of Solids Accumulation on the Floor (lbm/ft<sup>2</sup>) for the Case of 70  $\mu\text{m}$  Particles, 9.1 m (30 ft) Fluid Depth, and a Low Critical Shear Stress [ $\tau_d = \tau_r = 11 \text{ dyne/cm}^2$  (0.023 lbf/ft<sup>2</sup>)] Assumption

In each of these cases, if the floor density, divided by the density of the solids and a maximum packing factor, is used to obtain an estimate of the layer thickness, the layer of material would be quite thick. This indicates that the thin layer assumption of the floor resuspension deposition model coded into TEMPEST has been violated. The results in Figure 4.7, however, should be representative, because at the largest floor density value of 35 lbm/ft<sup>2</sup>, the layer would be roughly 2.5-cm (1-in.) thick. Furthermore, if credit is taken for the fact that only about 5% of the solids material in the tank will be greater than 50  $\mu\text{m}$ , the layer would be only be approximately 0.13 cm (0.05 in.) thick. Layer thicknesses of less than 2.5 cm (1 in.) would be within the validity of the thin layer assumption in the resuspension deposition model in TEMPEST.

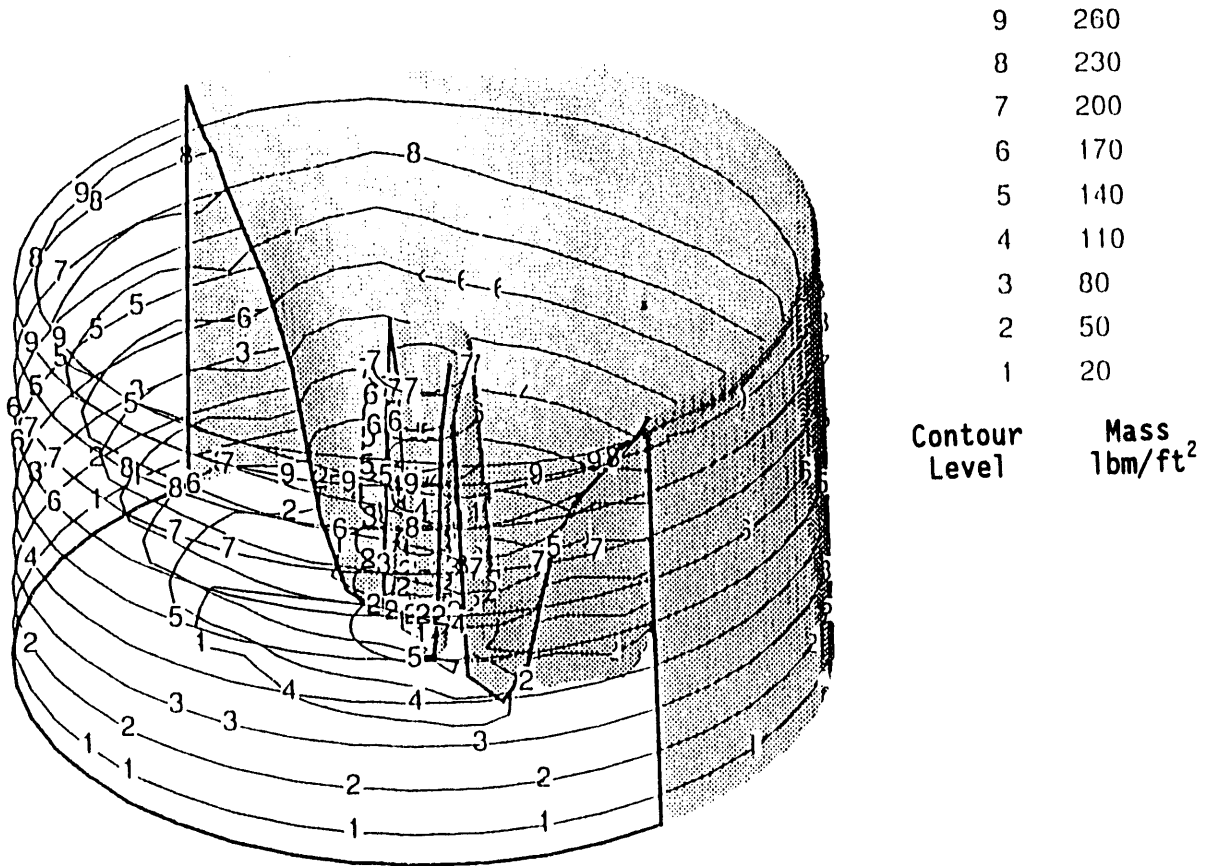


**FIGURE 4.8** Surface Representation of Solids Accumulation on the Floor (lbm/ft<sup>2</sup>) for the Case of 70  $\mu\text{m}$  Particles, 9.1 m (30 ft) Fluid Depth, and a Medium Critical Shear Stress [ $\tau_d = \tau_r = 96 \text{ dyne/cm}^2$  (0.200 lbf/ft<sup>2</sup>)] Assumption

The time dependence of the accumulation of material on the floor of the tank is shown in Figures 4.10 and 4.11 for the large particles (70  $\mu\text{m}$ ) and the small particles (10  $\mu\text{m}$ ) modeled. In each of the figures, the total mass of material accumulated on the floor is plotted as a function of time for three assumptions of critical shear stresses. Low [ $\tau_d = \tau_r = 11 \text{ dyne/cm}^2$  (0.023 lbf/ft<sup>2</sup>)] implies that all material along the axis of the jet is resuspended, medium [ $\tau_d = \tau_r = 96 \text{ dyne/cm}^2$  / 90.200 lbf/ft<sup>2</sup>)] implies that a portion of the material along the axis of the jet is resuspended and subsequently redeposited along the axis; and high [ $\tau_d = \tau_r = 358 \text{ dyne/cm}^2$  (0.747 lbf/ft<sup>2</sup>)] implies no material is suspended along the axis of the jet. Each of these cases were run

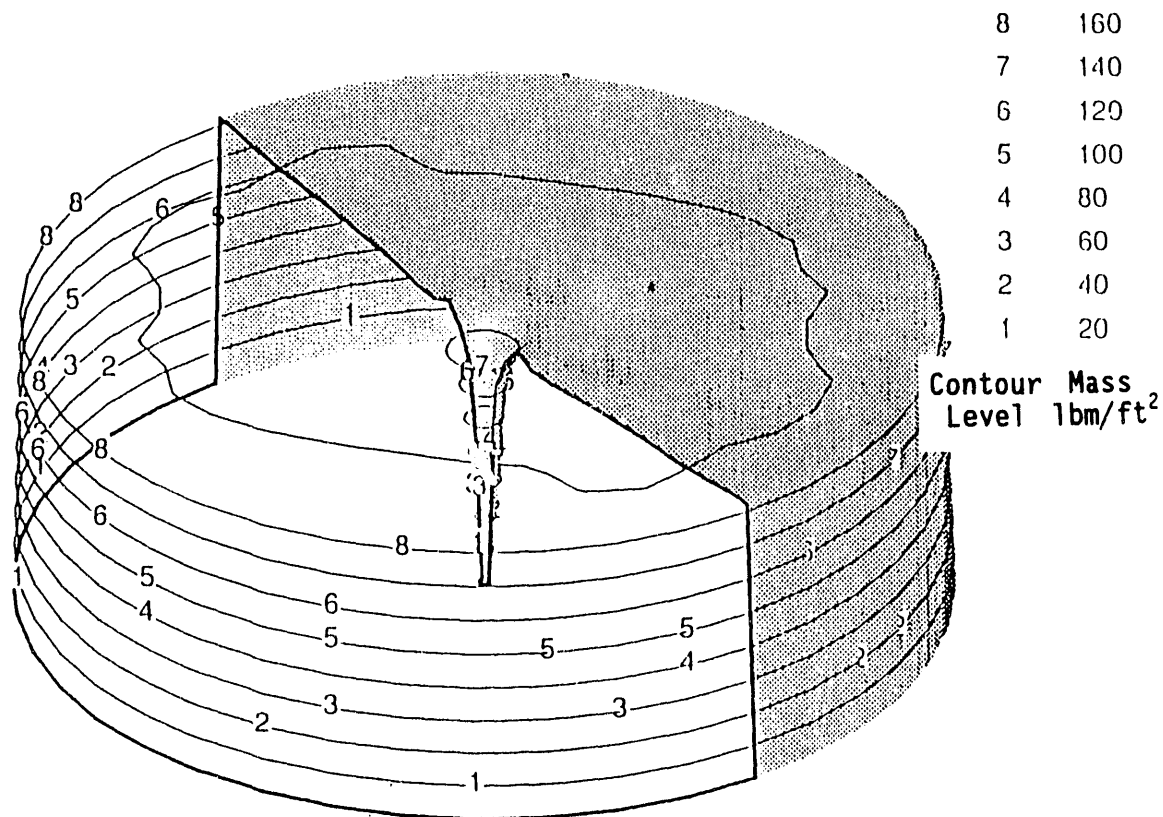


**FIGURE 4.9** Surface Representation of Solids Accumulation on the Floor (lbm/ft<sup>2</sup>) for the Case of 70  $\mu\text{m}$  Particles, 9.1 m (30 ft) Fluid Depth, and a High Critical Shear Stress [ $\tau_d = \tau_r = 358 \text{ dyne/cm}^2$  (0.747 lbf/ft<sup>2</sup>)] Assumption

for a fluid depth of 9.1 m (30 ft). For the case of large particles (Figure 4.10), if the material is not completely resuspended along the axis of the jet (medium and high  $\tau_d$  cases), eventually all of the material will be deposited somewhere on the tank floor. If all the material is resuspended along the axis of the jet as the jet sweeps by, an equilibrium condition is reached, even if it is redeposited somewhere else. The same is true for the small particles (Figure 4.11), although it would take longer for the small particles to accumulate on the floor. Figure 4.11 shows that only the low critical shear stress case has reached a state of quasi equilibrium, that is, a state where for each pump oscillation as much particulate material is reentrained as settles out.

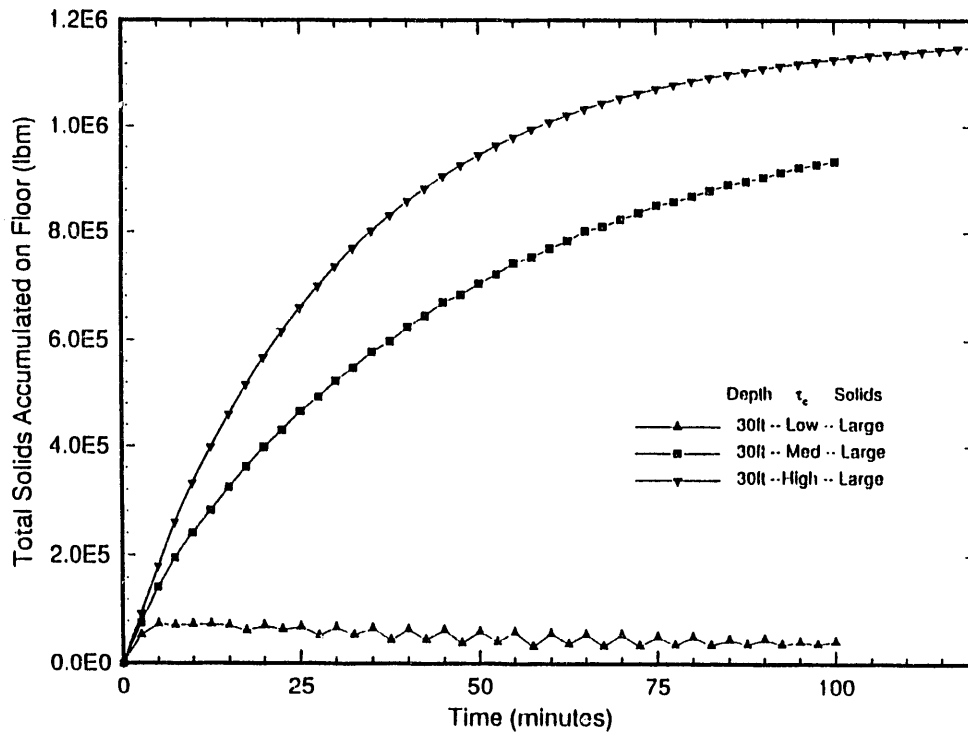


**FIGURE 4.10** Accumulation of Solids on Floor for Three Critical Stress Assumptions (Large Particles at 13 Wt% Solids)

The implication of these species transport results is that if the critical shear for resuspension of settled material is less than the turbulent shear stress along the axis of the floor jet over the longest distance a jet has to traverse, an equilibrium condition would exist wherein only a small fraction of the material in the tank would be on the floor at any given time.

Solids mass fraction distributions in the vertical direction at various locations around the tank are presented in Figures 4.12 through 4.14. These results are for the small particle (10  $\mu\text{m}$ ) cases computed with the three critical shear stress assumptions: low being a small enough value for all material to be picked up along the total length of the jet axis; medium being a value somewhere between the minimum and maximum of the distribution along the jet axis; and high being a value greater than the maximum of the distribution along the jet axis such that no material is resuspended.

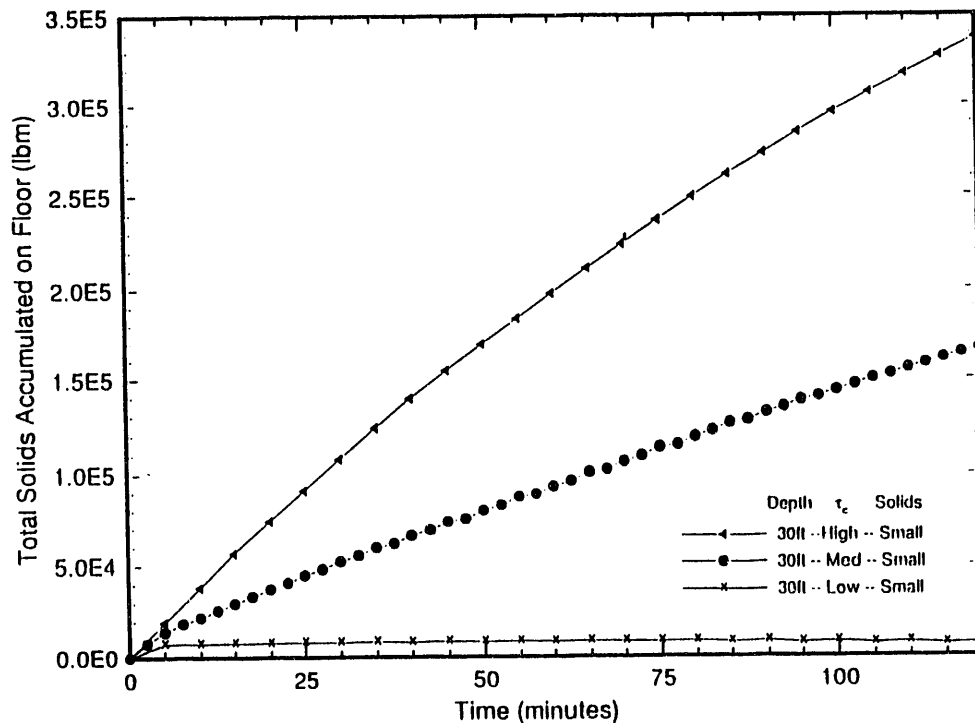


**FIGURE 4.11** Accumulation of Solids on Floor for Three Critical Stress Assumptions (Small Particles at 13 Wt% Solids)

In Figure 4.12 for the low critical shear stress assumption, there appears to be a rather large variation in the mass fraction at the different locations around the tank. Note that for this case, an equilibrium condition has been reached for the material that deposits on the floor between each passing of the jet (see Figure 4.11). All of the material deposited between jet sweeps is resuspended by the jet. As a result, the mass fraction adjacent to the tank wall and in a plane subtended by the jet axis (open circles) is quite high because of the material that has just been resuspended from the floor layer. Thus, except for the very localized region adjacent to the floor and up the outer wall in the plane of the jet axis, the variation in distribution of material around the tank is quite uniform, being less than about a 5% variation from the mean. A very similar effect is seen in Figure 4.13 for the medium critical shear stress assumption. For this case, some of

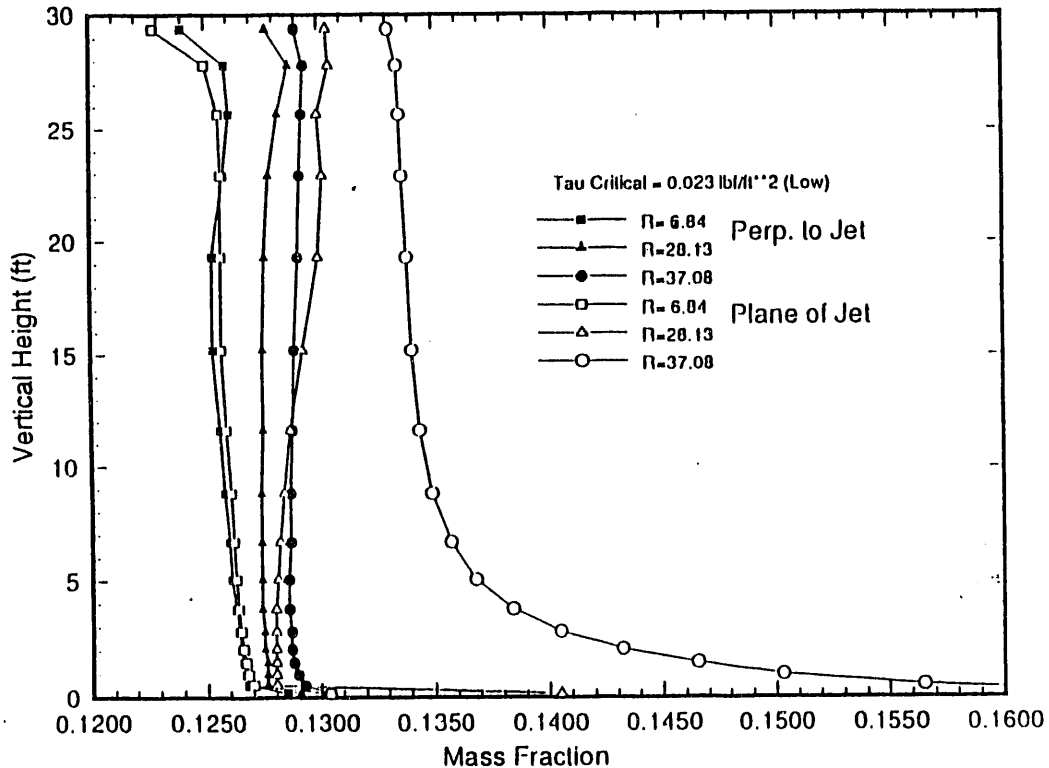


**FIGURE 4.12** Vertical Variation of Mass Fraction for Low Critical Shear Stress

the material deposited between jet sweeps is resuspended along the axis of the jet, but not all. Thus, the variation with position is not as marked. However, it must be noted that for this case, an equilibrium condition has not been reached either, because a net amount of material is depositing relative to resuspending (see Figure 4.11). Eventually, the "average" mass fraction of these curves will tend towards zero. Of primary significance here; however, is that there is less than about a 5% variation in material throughout the tank, except for the local effect caused by floor resuspension along the axis of the jet. This observation is further supported by results in Figure 4.14 for the high critical shear stress assumption where it is evident that no material is being resuspended along the jet axis. Again it is seen that the variation around the tank is less than about 5%.

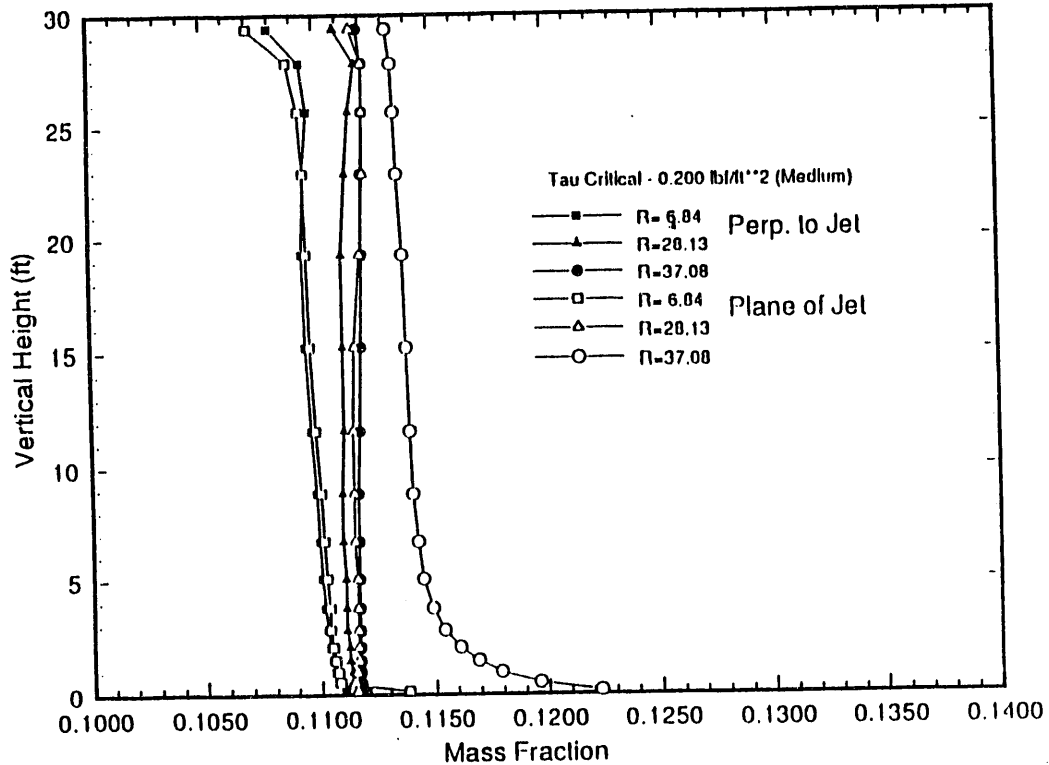


**FIGURE 4.13** Vertical Variation of Mass Fraction for Medium Critical Shear Stress

The primary significance of these species transport results is, again, a reaffirmation that the critical shear stresses for resuspension and deposition of particulate material are of "critical" importance. If, on the floor along the axis of the jet, there is sufficient turbulent shear stress developed to resuspend particulate material deposited between jet sweeps, the mixing pumps should be able to maintain material well mixed in the fluid volume, except for localized effects caused by resuspension along the axis of the jet.

#### 4.5 RESULTS OF SLOPED-FLOOR MODELING

Analysis of the effect of the sloped floor of the tank was conducted by two approaches: 1) investigate geometric considerations of the intersection of an (assumed) unconfined round free jet with an (assumed) sloping tank floor and 2) use TEMPEST to compute the hydrodynamics of mixing jets issuing from a

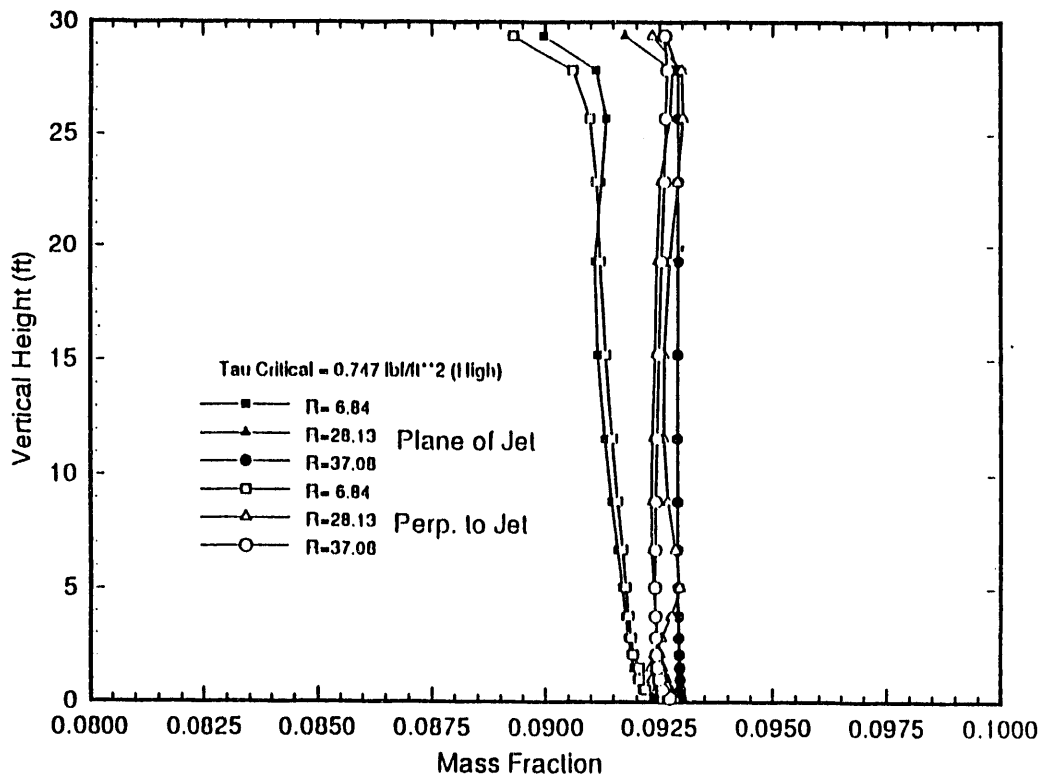
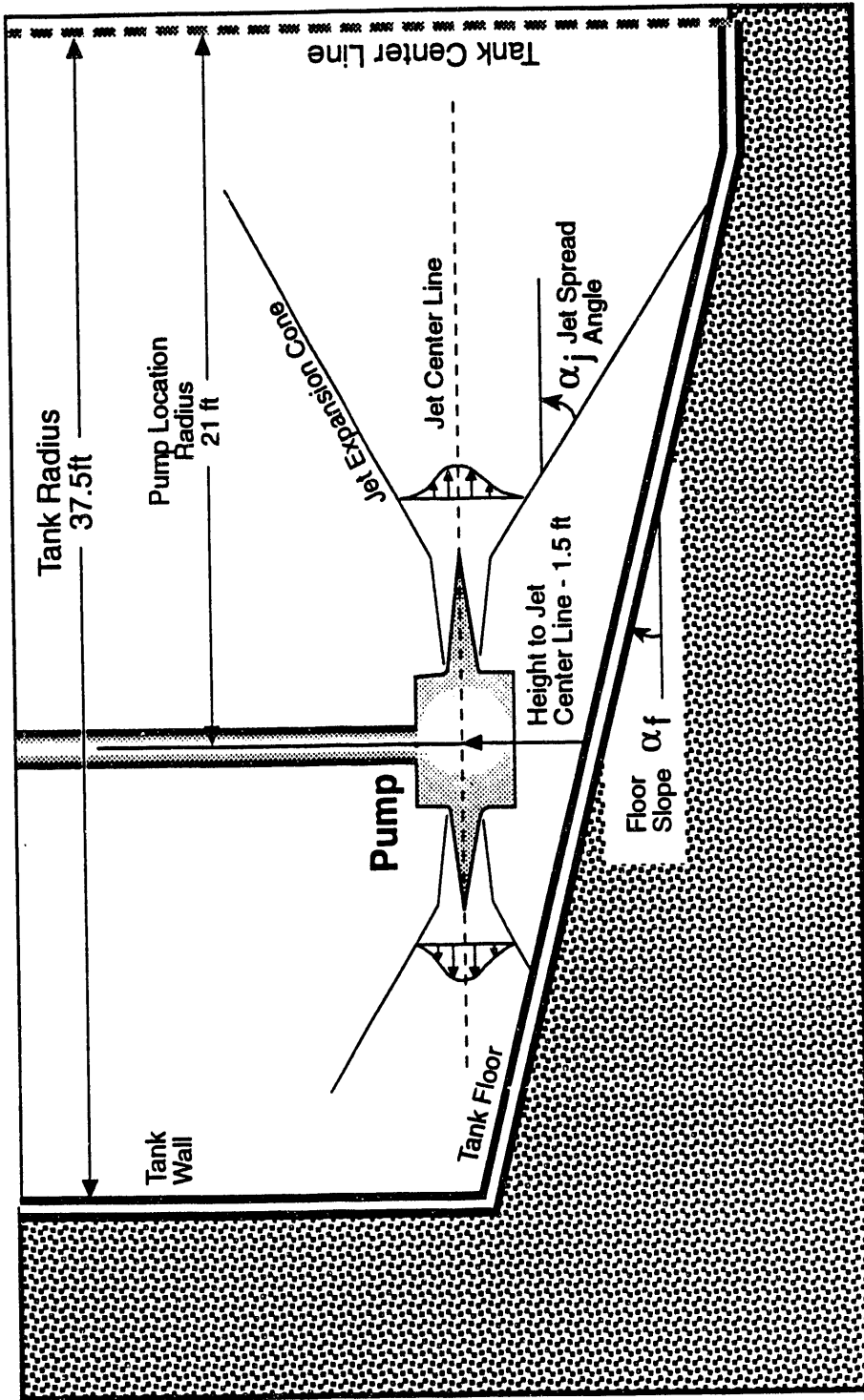


**FIGURE 4.14** Vertical Variation of Mass Fraction for High Critical Shear Stress

pump. In the latter approach, a single pump was assumed to be offset 6.4 m (21 ft) from the center of the tank. The hydrodynamics of the jets and the shear stress developed on the floor were of primary concern. One jet is directed at the nearest tank wall and the other is directed through the tank centerline at the far tank wall.

#### 4.5.1 Geometric Considerations

A schematic of a mixing pump located off center in the tank is shown in Figure 4.15. If a jet expansion cone angle for an unconfined free round jet is assumed (or known from an empirical correlation), it is mathematically possible to develop the equations for the intersection of the expansion cone and the sloped floor of the tank. When initially attempted, this approach produced an iterative solution of transcendental equations with very poor



Not to Scale

**FIGURE 4.15** Schematic of Geometric Consideration of Mixing Jets Issuing from a Single Mixing Pump Offset from the Tank Center and Located above a Sloping Tank Floor

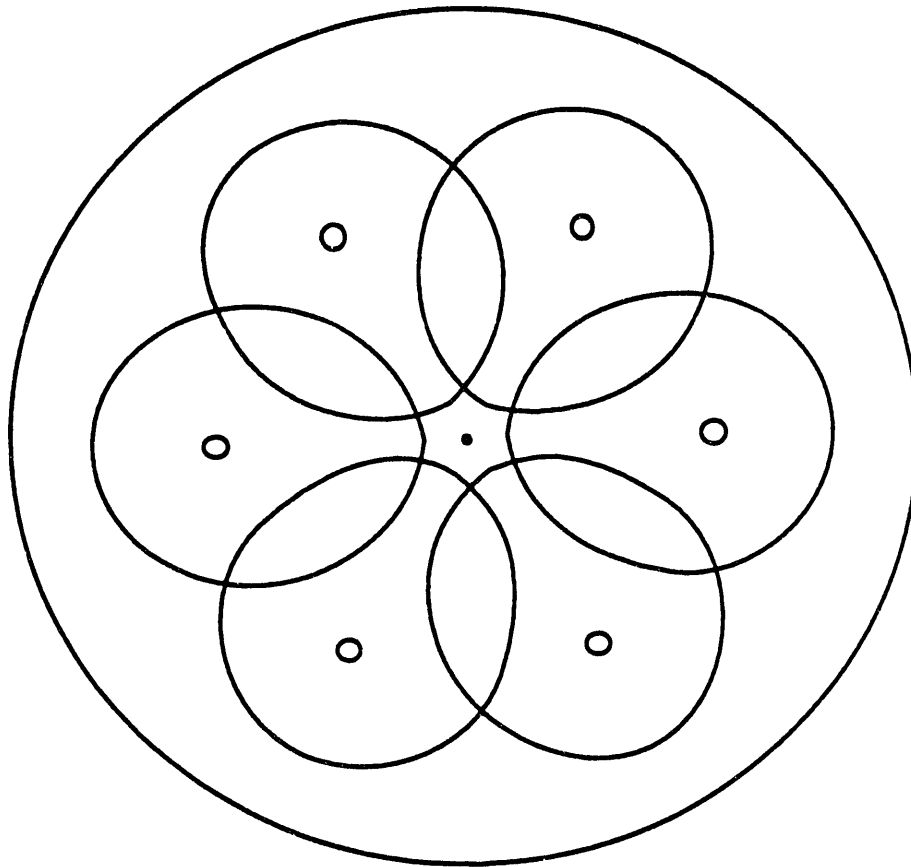


**FIGURE 4.16** Lines of Intersection of an Assumed Free Turbulent Jet with a Sloped Tank Floor (7 degree Jet Half Angle of Expansion and 3% Floor Slope)

convergence behavior; therefore, the approach was terminated. Instead, the intersection was obtained graphically using a solid body modeler on a computer. Results of the intersection curves for a six-pump in-tank configuration are presented in Figure 4.16 for a floor slope of 3% (1.7 degree).

A jet cone spread angle of 14 degree (7 degree half angle,  $\alpha_{j,1/2}$ ) was used in these results. This angle corresponds to a velocity ratio  $U/U_m = 0.31$ , where  $U$  is the local velocity at the edge of the jet cone spread and  $U_m$

is the local velocity at the jet centerline. This result is derived from an expression for an unconfined free jet (Abraham 1963) to be<sup>(a)</sup>

$$\tan(\alpha_{j,1/2}) = [\ln(1/f)/K]^{1/2} \quad (4.6)$$

where  $f$  equals  $U/U_m$ , the local velocity ratio, and  $K$  equals 77, an experimentally determined constant.

Data in Figure 4.16 indicate that there is sufficient overlap of the floor sweeping effect of the jet to adequately cover the whole of the floor with six pumps. In fact, the  $U/U_m = 0.31$  line is probably very conservative because in the real case of the confined floor jet, attachment and hence sweeping action would be a much tighter circle. This is because a wall (floor in this case) confined jet will tend to deflect slightly<sup>(b)</sup> because of reduced entrainment caused by the presence of the floor. This geometric analysis approach, however, does not address whether the turbulent shearing action of the floor jet is sufficient to cause resuspension of any settled material.

#### 4.5.2 Description of Computer Modeling Approach

A computer modeling approach was used to further investigate the effect of the slope floor. This was done by simulating two jets issuing from a single pump located at a distance of 6.4 m (21 ft) from the tank centerline (see Figure 4.15). For this simulation, the centerplane of the tank was assumed to be of primary importance, and thus the calculation was performed in a large, rectangular volume representing the tank. The pump was assumed to be stationary with the axis of one of the fluid jets directed towards the nearest wall and the other directed through the tank center towards the opposite wall. For these assumptions, the characteristics of the axial floor jet could be

---

(a) Internal correspondence from DS Trent, Pacific Northwest Laboratory to RT Allemann, Pacific Northwest Laboratory, dated March 18, 1992.

(b) L. L. Eyler. 1988. Investigation of Coanda Deflection of Double Shell Tank Retrieval Process Mixing Jets. ESD-88-112, Rev 1. Internal report of work performed by Pacific Northwest Laboratory for Westinghouse Hanford Company.

investigated for both the up-slope and down-slope directions along the tank floor. The up-slope direction is of significance in that this is the direction of shortest distance to a tank wall. The down-slope direction is of significance because it represents the longest distance to a tank wall from a pump location. These two distances bound the length over which the jets from any single pump in the six-pump configuration would traverse along the tank floor.

Four calculations were conducted:

- flat bottom tank (for basis of comparison)
- 5% (3.0 degree) slope with the jet centerline at 0.46 m (1.5 ft) above the tank floor at the pump location
- 3% (1.7 degree) slope with the jet centerline at 0.30 m (1.0 ft) above the tank floor at the pump location
- 3 percent (1.7 deg) slope with the jet centerline at 0.30 m (1.5 ft) above the tank floor at the pump location.

The last of these cases is the design basis. The others were conducted as parameter investigations. For the sloped bottom cases, the generalized curvilinear coordinate feature of TEMPEST was used. In the computer model, the floor of the tank sloped down towards the tank center from under the pump location, across a 0.61 m (2 ft) flat surface at the tank center, and sloped up towards the opposite tank wall.

#### 4.5.3 Hydrodynamic Results

Results in Figure 4.17 compare the horizontal velocity component distribution as a function of height at the centerline of the tank. It is apparent that the cases of the steeper slope [5%,  $H_j = 0.46$  m (1.5 ft)] and shallower slope with the pump closer to the floor [3%,  $H_j = 0.30$  m (1.0 ft)] are less developed into floor jets than are the other two cases. This results in a lesser shear stress along the down-slope floor for these two cases, as shown in Figure 4.18. The up-slope side shows a significantly increased shearing action. These results are interpreted to indicate that for a six-pump configuration if the jets issue horizontally, the center of the tank has a greater propensity to accumulate particulate material because that is the

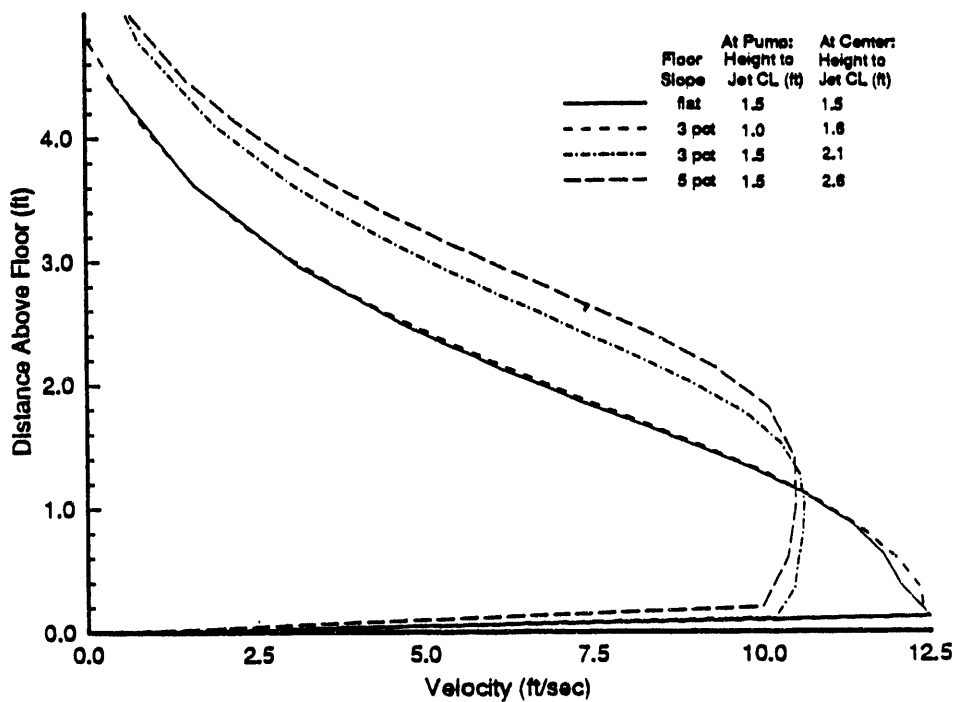


**FIGURE 4.17** Comparison of Horizontal Velocity Profile at the Tank Centerline of a Flat Bottom and Three Sloped Bottom/Pump Location Combinations for a Pump Situated at a 6.4 m (21 ft) Radius

region where the least shear stress exists for the resuspension of settled material. Actual accumulation, however, will depend upon the ratio of the critical shear for deposition relative to results such as those shown in Figure 4.18. A characteristic velocity field for the flat bottom case is shown in Figure 4.19.

#### 4.6 EXTENSION OF RESULTS TO SIX-PUMP DESIGN

The limitation in the TEMPEST code that a rotating pump could only be treated as centrally located requires that the results of the computer analysis be extrapolated to the six-pump design. Doing so requires some heuristic modeling, some extension of results, and some comparative discussion. There are three basic areas in which this has to be done: 1) hydrodynamic mixing enhancements of the six-pump configuration, 2) physical

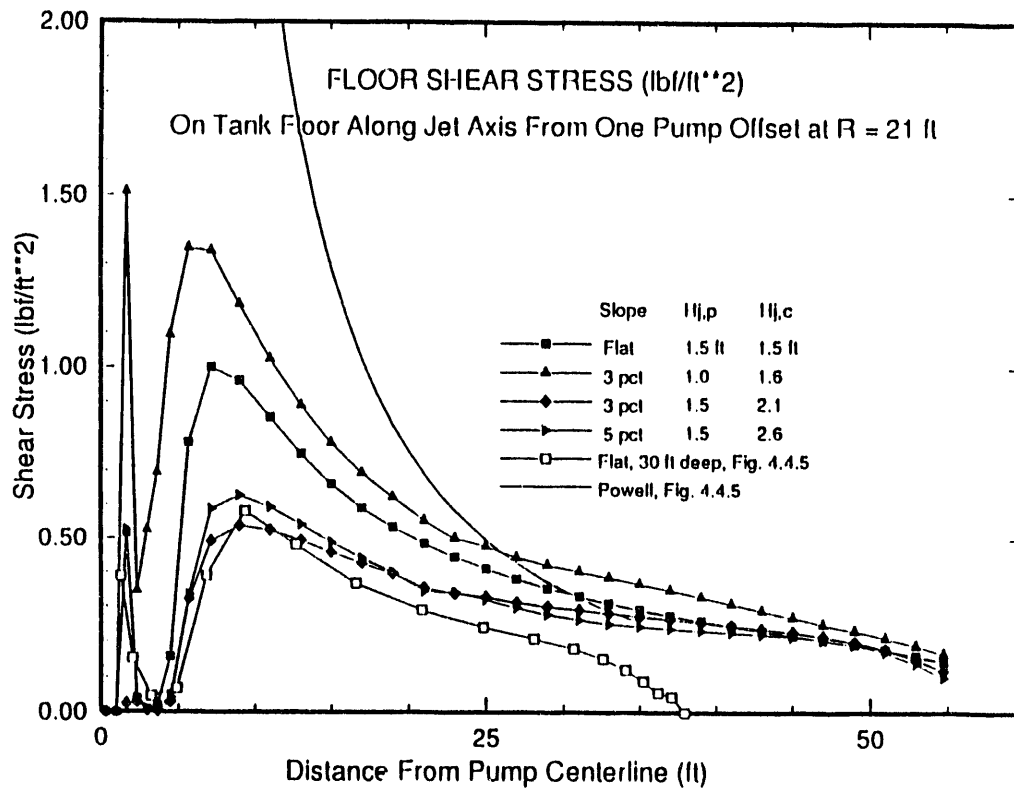


**FIGURE 4.18** Comparison of the Downward Slope Direction Turbulent Shear Stress Distribution on the Floor of the Tank Along the Axis of the Jets of a Flat Bottom and Three Sloped Bottom/Pump Location Combinations for a Pump Situated at a 6.4 m (21 ft) Radius

processes of solid-liquid interactions, and 3) special considerations of problems that a six-pump configuration would induce that a single pump would not.

#### 4.6.1 Fluid Hydrodynamics of the Mixing Process

The single pump results indicate quite clearly from the smaller (10  $\mu\text{m}$ ), lighter (specific gravity of 1.6), particle analysis that the jet convective action is quite capable of circulating the solid particles throughout the tank volume and maintaining the material well mixed. The caveat to this observation is that material that is deposited on the floor, in whatever fraction of the total, will induce a local perturbation to the uniformity of the distribution. This perturbation will be in the form of a locally higher

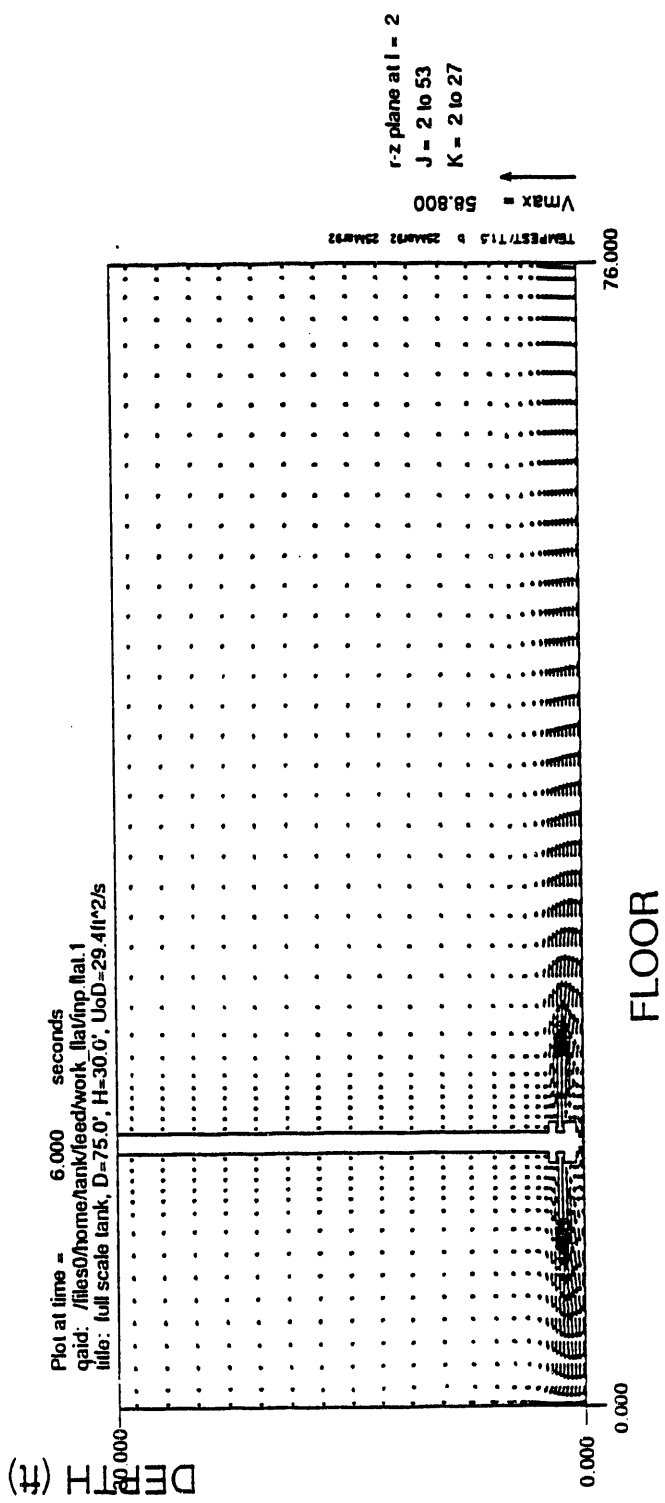


FIGURE 4.19 Characteristic Velocity Profile for Three-Dimensional Flat Bottom Model

concentration near the (axial) end of the jet caused by material resuspended along the jet's axial path. The logical extension of this result is that six pumps will do just as a good, if not better, a job of reducing the amount deposited.

The results of the fully coupled hydrodynamics with the settling and density effects of the larger (70  $\mu\text{m}$ ) particles modeled with a specific gravity of three indicate potential for the jet to become a forced plume (e.g., lift off the floor) if all the solid particle material in the tanks are at these parameters. For the six-pump case, which possesses six times the pumping power of the single jet case, it can be rationally argued that each pump would see only 1/6th of the same material and the settling effects on the jet would be reduced accordingly. Furthermore, the material particle size distribution of an actual waste (such as neutralized current acid waste) is expected to have only 5% of its content in the 50  $\mu\text{m}$  size range and greater. This further reduces the propensity for density effects to significantly alter the hydrodynamics of the floor jet.

At low liquid levels in the tank, flat-bottom tank analysis indicated that there was a jet entrainment hindering mechanism present caused by proximity of the free surface. From these observations, it is concluded that there would be an overall advantage to tilting the pump (or otherwise angling the jets) so that each of the jets issues into the fluid parallel to the floor at all rotation angles. The down side is that at low liquid levels, the jet may impinge at a right angle on the nearest wall to be diverted upward by the tank knuckle with sufficient momentum to induce significant surface penetration. This may be of significance to concerns of aerosol generation in the dome space.

#### 4.6.2 Resuspension and Deposition

This analysis was done with little confidence that the absolute values of the critical shear stress for resuspension (in particular) are directly applicable to particulate material that is expected to be present in the feed preparation tank. For that reason, the analysis parameterized the effects as a function of the critical shear stress relative to the maximum and minimum along the floor jet axis. The results indicated that IF the critical shear

stress for resuspension was less than the minimum along the floor jet axis, all material deposited on the floor between jet passings would be resuspended during the sweep. If the critical shear stress were somewhere between the minimum and maximum, some material would be picked up, but only to be redeposited further along. If the critical shear stress for resuspension is greater than any turbulent shear stress along the jet axis, no material would be resuspended. Thus, it would be prudent to do a more exhaustive study to quantify the critical shear stress as it applies to the DST tank wastes.

In spite of this uncertainty, several arguments can be made regarding the relation of the single pump modeling to the six-pump design. From just a geometric point of view, the maximum distance along which a single jet from the six pump/12 jet design would have to traverse would be 6.7 m (22 ft) (see Figure 3.3). For a scenario where only three of the jets were operating, the maximum distance would be 9.9 m (32.5 ft). (This distance is roughly the same distance from a centrally located pump to the tank wall.) Discounting the potential for a shadowing/interference effect of a disabled pump in between the two, the single, centrally-located pump results would be the same as far as resuspension along the jet axis is concerned. Again, material could be resuspended as long as the critical shear for resuspension was greater than the minimum of the distribution along the jet axis (see Figures 4.6 and 4.18).

Another consideration would be that the net amount of material which would need to be deposited/resuspended per pump would be 1/6 that of the single pump analysis. For the six-pump case, at equilibrium, the mass flux depositing (Equation 4.3) would have to be less than or equal to that being resuspended (Equation 4.4). Mathematically, for the conservative case of the critical shear stress for deposition being equal to that for resuspension (e.g., no hysteresis), the relation becomes

$$\rho_m V_s \phi A_d t_d \leq R A_j (1-t_d). \quad (4.7)$$

The product,  $\rho_m \phi$ , is the mass concentration of solids in units of mass per volume,  $A_d$  is the depositing (settling) area, and  $A_j$  is the area swept by the jet. Note that  $A_d = A_T - A_j$ , where  $A_T$  is the total floor area of the tank and  $t_d$  is the time interval between jet sweeps at a given location. This time is

a function of jet width because the jet is spreading as it traverses along the tank floor. Thus, if one ascertained that the resuspendability of settled material in the tank was of sufficient value as to exceed the average mass concentration times the settling rate (Stokes settling velocity, Equation 4.1), and the ratio of the area times the time over which deposition was occurring relative to that over which resuspension were occurring, it could be argued that no net material would accumulate on the floor. The deposition and resuspension regions are shown schematically in Figure 4.20. To obtain a closed solution of the criterion of Equation (4.7) requires an expression for the spread of the floor jet, or an area integration of floor shear contours such as those shown in Figures 4.3, and a rather complicated (geometrically) integration. This approach to analyzing the tendency for net build up of material on the floor with time was not completed because it was concluded that a more in-depth understanding of the resuspendability would be necessary to make the effort worthwhile.

#### 4.6.3 Special Considerations of the Six-Pump Design

There are at least two special considerations that have to be given to the six-pump design that were not analyzed directly. One is the potential for jet interference from adjacent pumps, and the other is the effect of the floor jet impinging at an angle other than normal to the tank wall. Such an impingement angle would be near that shown in Figure 4.20.

Floor jets from adjacent pumps will intersect as the pumps rotate through an oscillation. It is conceivable that if the pumps are rotating synchronously, and their jets are aligned in one of several ways, the ability of the floor jets to continuously sweep the whole of the tank floor may be impeded by the jets interfering with each other. To counter this potential, it is suggested that the pumps be rotated asynchronously with perhaps two or three rotation rates.

The effect of the jets impinging on the tank wall at an angle other than normal has not been analyzed. An intuitive argument can be made, however, that this will not have a major impact on the design. Consider a jet angle such as shown in Figure 4.20. Upon reaching the tank wall, the floor jet will

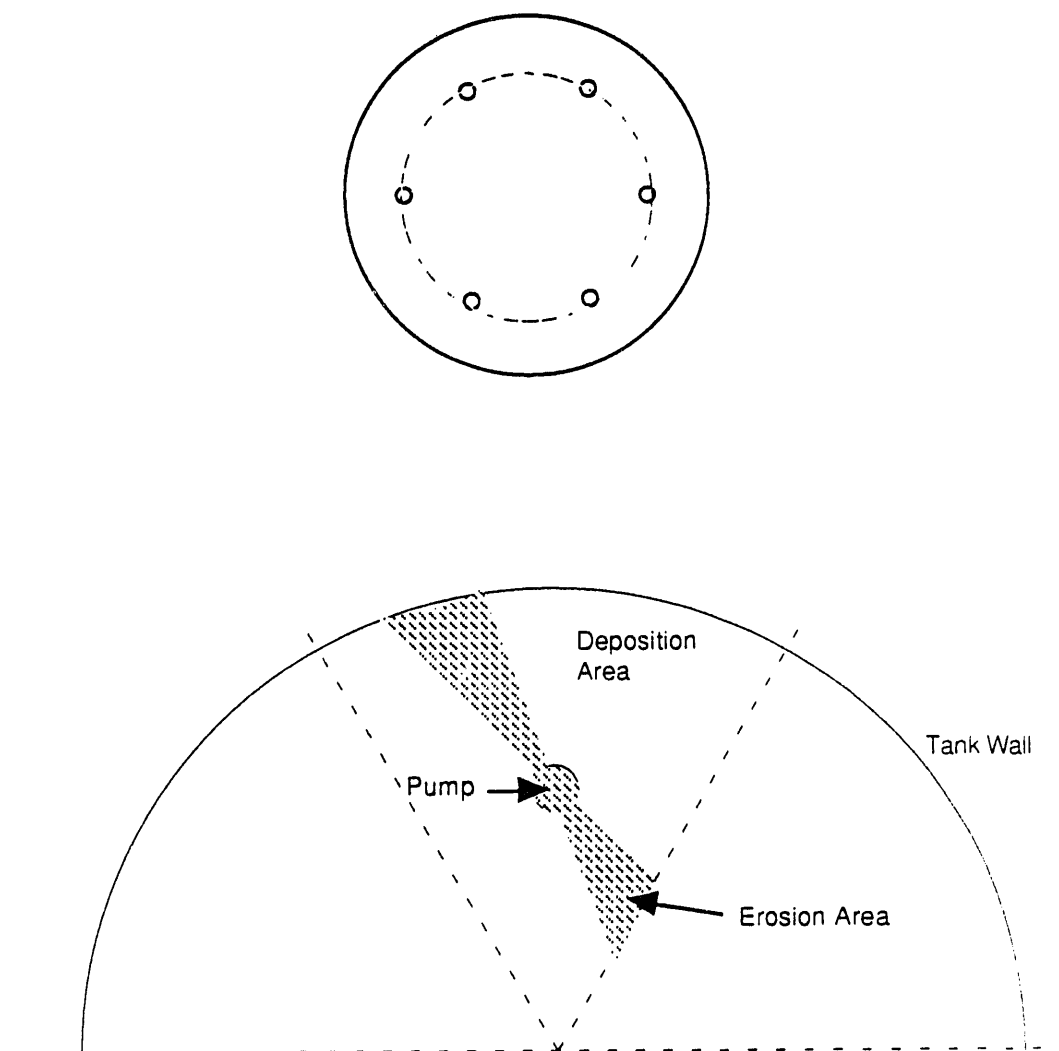


**FIGURE 4.20** Schematic of Deposition and Resuspension Areas on the Floor of a Six-Pump Design

be partially diverted upward by the tank knuckle and be partially diverted in the azimuthal direction. Any portion of the diversion up the tank wall will aid in mixing material resuspended from the floor. Any diversion azimuthally around the tank wall will carry material further towards a position where another jet from an adjacent pump will pick it up and move it back. It is this back and forth (washing machine) action that is arguably the mechanism that would keep it suspended.

## 5.0 OPERATIONAL AND DESIGN CONSIDERATIONS

Operational considerations for mixing pumps and retrieval pumps are discussed in Section 5.1. In Section 5.2 parameters that affect mixing uniformity are investigated to suggest alternative mixing and retrieval pump operating strategies.

### 5.1 MAINTAINING UNIFORM CONCENTRATION IN THE HWVP PROCESS FEED STREAM

Operating the HWVP feed preparation system to provide a feed stream where concentration remains within specified concentration limits is of extreme importance. There are two complementary methods to provide a uniform process feed: 1) maintain a uniform concentration throughout the tank within feed specifications or 2) withdraw the feed at a location within the tank that stays within the specified concentration.

#### 5.1.1 Mixing Pump Operation

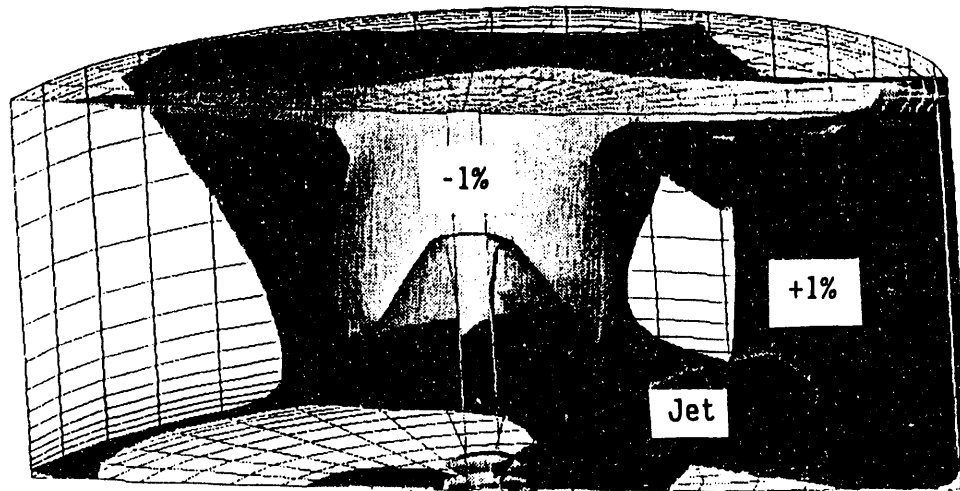
The operating specifications for the concentration uniformity of the HWVP feed stream have not been finalized. Several homogeneity goals and corresponding ranges in concentration have been proposed as listed in Table 5.1. The more reasonable homogeneity requirement for a 3875 m<sup>3</sup> (1-million-gal) tank is probably a homogeneity of 80% to 90%.<sup>(a)</sup>

TABLE 5.1 Proposed Homogeneity/Uniformity Specifications

<u>Homogeneity</u>	<u>Top-to-Bottom Concentration</u>
98%	±1%
95%	±2.5%
90%	±5%
80%	±10%

---

(a) L. D. Swenson. October 24, 1991. "Hanford Waste Vitrification Plant Feed Tank Agitation Assessment." Memo 85433-91-067. Westinghouse Hanford Company, Richland, Washington.



**FIGURE 5.1** Constant Concentration Contours (-1%, Mean, +1%) for Homogeneity of 98% for 10- $\mu$ m Particulate at a Fluid Depth of 9.1 m (30 ft)

In this analysis, computational results were based on a single, centered, rotationally-oscillating, dual-jet mixer pump. Data from this configuration were analyzed to observe the regions of tank volume that exhibit these degrees of homogeneity for 10- $\mu$ m diameter particulate at a fluid depth of 9.1 m (30 ft). Surfaces of constant concentration  $\pm 1\%$ ,  $\pm 2\%$ , and  $\pm 5\%$  uniformity are plotted in Figures 5.1 through 5.3. These are isocontours of concentration. Unshaded regions are simply not of the specific concentration level. For points between the contours, the concentration should be within the specified bounds; for points outside of the contours, the concentration will be outside the specified bounds. In each of these figures the jet is shown in black. The lighter shaded dots at the top center of the plot indicate an isosurface of concentration at the lower tolerance (-1%, -2%, or -5%) from the mean concentration. The darker shaded surface at the lower portion and along the wall of the tank indicates an isosurface of concentration at the higher tolerance (+1%, +2%, or +5%) from the mean concentration. These figures show that most of the fluid in the tank is within  $\pm 1\%$  of the mean concentration, and virtually all of the fluid is within  $\pm 5\%$  of the mean. For ease of interpretation, the mean concentration has been

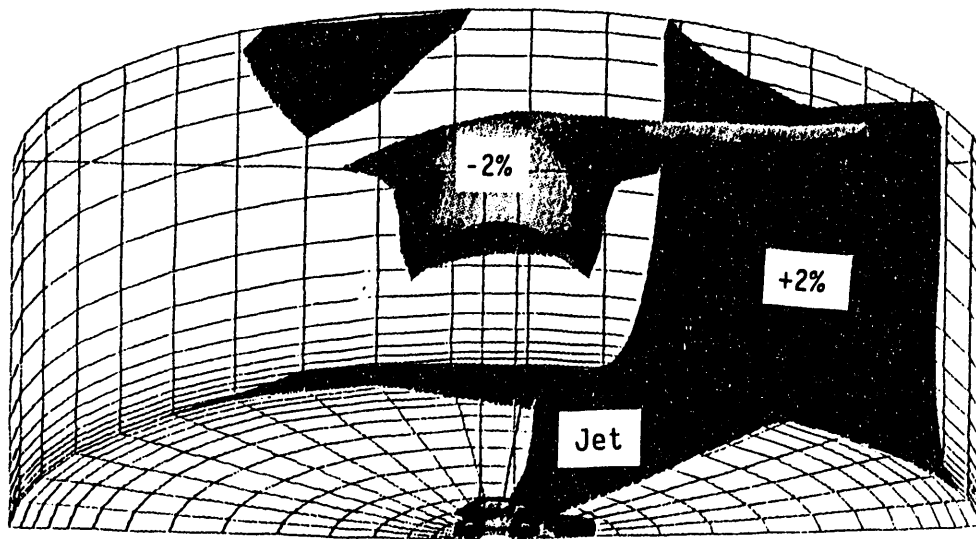


**FIGURE 5.2** Constant Concentration Contours (-2% and +2%) for Homogeneity of 96% for 10- $\mu\text{m}$  Particulate at a Fluid Depth of 9.1 m (30 ft)

omitted from Figures 5.2 and 5.3. The volume between these surfaces is within the specified homogeneity. The area of the lower boundary along the floor beneath the jet and along the tank wall indicates areas where the jet is resuspending particulate that is being carried to the upper surface of the tank. The plots show that for 10- $\mu\text{m}$  diameter particulate in a tank filled to a fluid depth of at 9.1 m (30 ft) the majority of the tank remains uniform within the  $\pm 5\%$  isosurface of concentration.

### 5.1.2 Retrieval Pump Operation

The location of the inlet to the transfer pump, used to retrieve feed from the tank, may influence the uniformity of the feed stream. The maximum degree of inhomogeneity achieved during retrieval will differ from the spatial inhomogeneity in the tank as will be demonstrated in the following examples.

Concentration profiles of settling solids in turbulent flows may be estimated by an exponential function, particularly when the mechanism for distributing the solids is diffusive (Bamberger, Liljegren, and Lowery 1993). Typical concentration profiles showing the manner in which the solids concentration will vary with the fractional height from the bottom of the tank

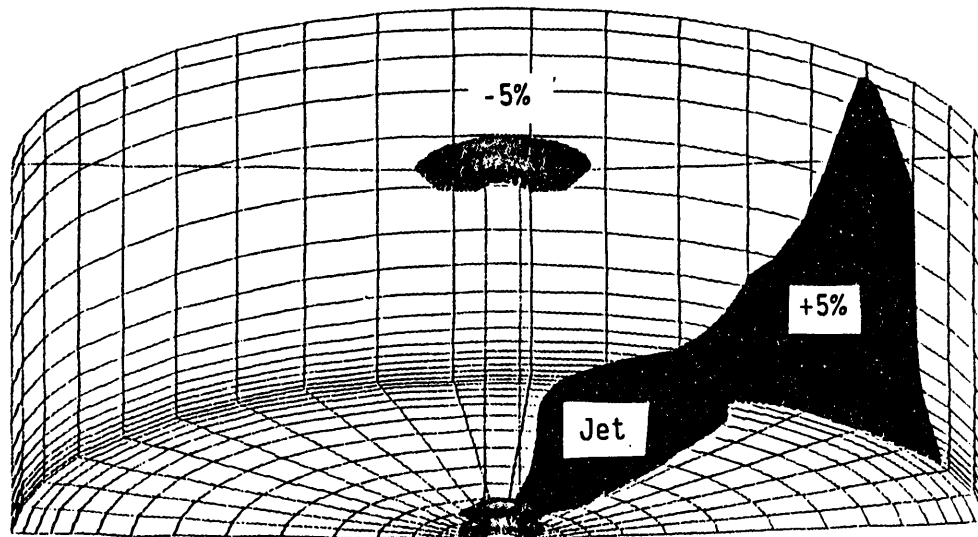


**FIGURE 5.3** Constant Concentration Contours (-5% and +5%) for Homogeneity of 90% for 10- $\mu\text{m}$  Particulate at a Fluid Depth of 9.1 m (30 ft)

are shown in Figure 5.4 based on the assumption of an exponential profile. The concentration as a fraction of mean solids concentration in the tank is illustrated for three cases: concentrations variations from top to bottom of  $\pm 1\%$ ,  $\pm 10\%$ , and  $\pm 100\%$  of the mean concentration.

In Figures 4.12 through 4.14, vertical variation of mass fraction was presented for three levels of critical shear stress: low, medium, and high. These plots were based on a fluid depth of 9.1 m (30 ft) and 10- $\mu\text{m}$  diameter particulate. The plots present mass fraction as a function of elevation at three radii, in a plane parallel to the jet and a plane perpendicular to the jet. At each snapshot in time, the mass fraction variations are quite constant with elevation. Therefore, based on these examples at full fluid depth, the radial location of the retrieval pump is not critical.

Although it is not certain that an exponential function may describe the solids distribution during suspension of solids throughout the tank as a function of fluid height, an analysis to determine the typical variation in the concentration at the withdrawal point during retrieval was performed based on this profile. For each concentration profile, there is a tank location at which the concentration matches the mean concentration in the tank.

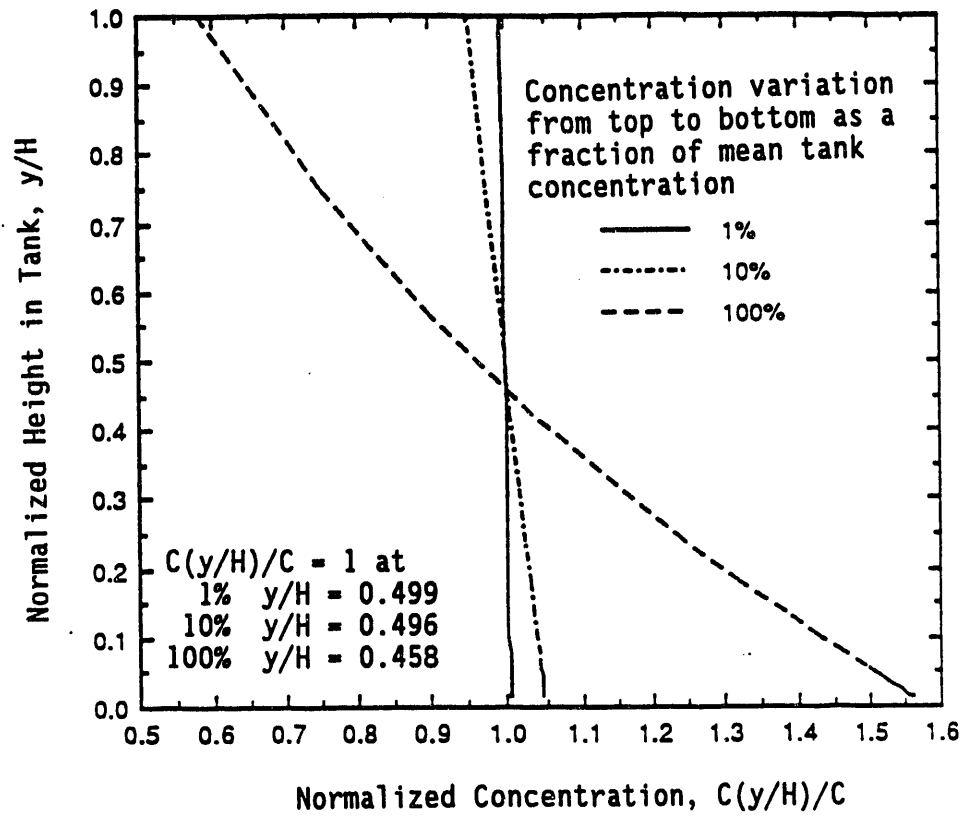


**FIGURE 5.4** Estimated Concentration Profiles as a Function of Height

Slurry withdrawal from this location would have the same concentration as the entire average tank concentration; this location might be considered to be the optimum location for withdrawal of slurry. This optimum site occurs at a distance from the bottom of the tank that depends on the degree of inhomogeneity in the solids concentration. When solids inhomogeneity is small, the optimum occurs at a horizontal plane passing through the tank center; when the inhomogeneity is large, the optimum occurs lower in the tank. The variation of the optimal withdrawal location as a function of the concentration difference between the top and bottom of the tank is shown in Figure 5.5.

Further analysis based on the assumption of an exponential profile to estimate concentration variation with height were conducted. The relations describing the spatial concentration profile were used to estimate variation

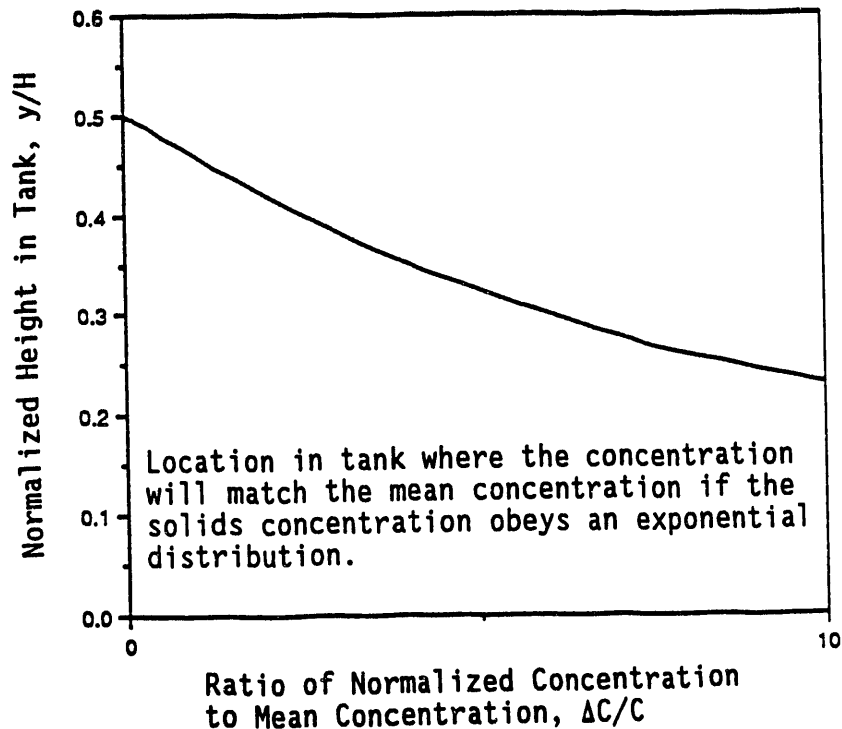


**FIGURE 5.5** Optimum Retrieval Location as a Function of Inhomogeneity

in the mean concentration in the tank and the variation in the concentration of feed as a function of feed level (Figure 5.6). In this example, solids were withdrawn from an elevation of  $0.25 H$ ,<sup>(a)</sup> where  $H$  is the initial liquid level in the tank; the initial concentration difference between top and bottom of the tank was 10%. The concentration of the retrieved slurry was found to be 2.5% greater than the average tank slurry concentration during initial stages of retrieval. This concentration fell as the tank emptied. The calculation was terminated when the liquid level dropped to the withdrawal point. During withdrawal, the mean concentration also varies with time. Initially the point at which feed is withdrawn from the tank is below the location of average concentration. As a result, the feed withdrawn from the

---

(a)  $0.25 H$  is an arbitrarily selected location. However, at this elevation  $0.75 H$  of the tank can be retrieved without a change in suction location, making the analysis at this location more desirable than a location above the tank mid-elevation.

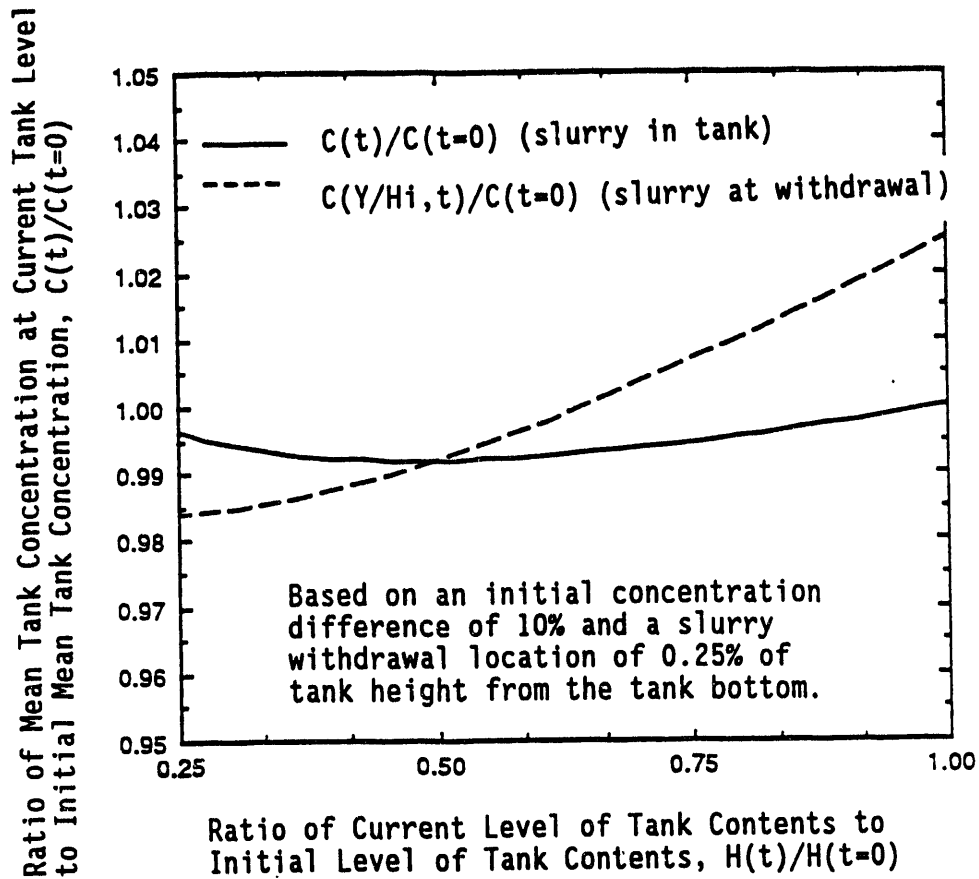


**FIGURE 5.6** Variation in Feed Density as a Function of Remaining Feed Height

tank is more concentrated than the average concentration in the tank and the overall feed concentration within the tank decreases with time. However, once the tank feed level falls sufficiently, the withdrawal location is above the location at which the local average matches the tank average. At this point the concentration of the withdrawn slurry is less than the average concentration of the feed within the tank and the concentration of the feed within the tank increases. The concentration of the retrieved feed when the tank feed level reaches the withdrawal location is slightly greater than 98%. Thus, although the original spatial variation in the tank contents was 15%, the variation in the concentration of the retrieved feed is approximately 4%.

These examples have shown the linkage between tank concentration, retrieval location, and feed concentration. The variation in the

concentration of the retrieved feed and the spatial variation in the concentration of feed remaining in the tank differ substantially. These differences will depend on the location of the retrieval port. Experiments to quantify the effects of retrieval port location are planned as a part of the double-shell tank retrieval project (Bamberger, Liljegren, and Lowery 1993).

## 5.2 DESIGN CONSIDERATIONS

Parameters that affect the uniformity of the tank contents and consequently the uniformity of the feed stream removed from the tank include

- physical properties of the process feed
  - concentration
  - particle diameter
  - slurry viscosity
  - densities of the supernatant, mixture, and particulate
  - yield strength
  - critical shear stress
- geometric parameters
  - number of mixing pumps
  - mixing pump location (radius, elevation, and angle to floor)
  - placement and diameter of mixing pump suction and nozzle
  - retrieval pump location (radius and elevation)
  - retrieval pump inlet diameter
  - depth of fluid
  - slope of floor
- dynamic parameters
  - jet rotation rate
  - jet asynchronization
  - jet nozzle exit velocity and discharge parameter ( $U_0D_0$ )
  - number of jets in operation at one time.

Based on the computational and heuristic analyses presented to date, observations regarding changes in some of these parameters are addressed.

### 5.2.1 Physical Properties

The particulate characteristics of density and diameter consolidated in the particle settling velocity probably have the greatest effect upon maintenance of uniformity with mixing pumps. The particulate diameter may be regulated by preprocessing activities prior to insertion into the HWVP feed preparation tank to reduce the particle diameter to one that can be maintained in suspension by the mixing pumps.

For particulate that has settled and must be mobilized, the critical shear stress for resuspension is the most important parameter. This parameter is more difficult to characterize than particle settling velocity and no method for its selective control is offered. Rheological investigations must be conducted to better quantify this parameter.

### 5.2.2 Geometric Parameters

Of the geometric parameters, the number of mixing pumps is most critical to the design. By reducing the number of mixing pumps, benefits are gained in two areas: 1) cost savings from purchasing, powering, decontaminating, and decommissioning less mixing pumps; and 2) decreased heat input to the tank from the mixing pump motors. One four-pump design that could be considered includes one centrally located mixing pump and three mixing pumps located on a 5.7 m (18.75 ft) radius 120 degrees apart is shown in Figure 5.7. A planar view schematic of the pump locations and geometric parameters such as linear distance to adjacent pumps is shown in Figure 5.8. In this design, with all four jets operating, the three offset jets must maintain a critical shear stress for resuspension for a length of 9.9 m (32.5 ft). Review of Figure 4.18 shows that over the region from 6.7 to 9.9 m (22 to 32 ft) floor shear stress remains relatively constant. Therefore, extending the working distance of each jet from 6.7 m (22 ft) for the six-pump design to 9.9 m (32 ft) for the four-pump design may be rationalized. Also placing a mixing pump at the tank center may inhibit accumulation of particulate in this region from offset jet interactions.

Some benefit may be obtained by mounting each mixer pump at an angle with the tank dome (through placement of a spacer) to orient the jet parallel to the tank floor. In this orientation, each jet would be able to resuspend equally effectively. In the current orientation, the up-slope jet may be more effective than the down-slope jet.

Depth of fluid is seen to have a profound effect on the shape of the jet. In this analysis three fluid heights were investigated; at the lowest depth, the jet did not achieve a floor jet profile. Restricted entrainment both above and beneath the jet caused it to assume more azimuthal rather than floor jet characteristics. When this transformation is considered in

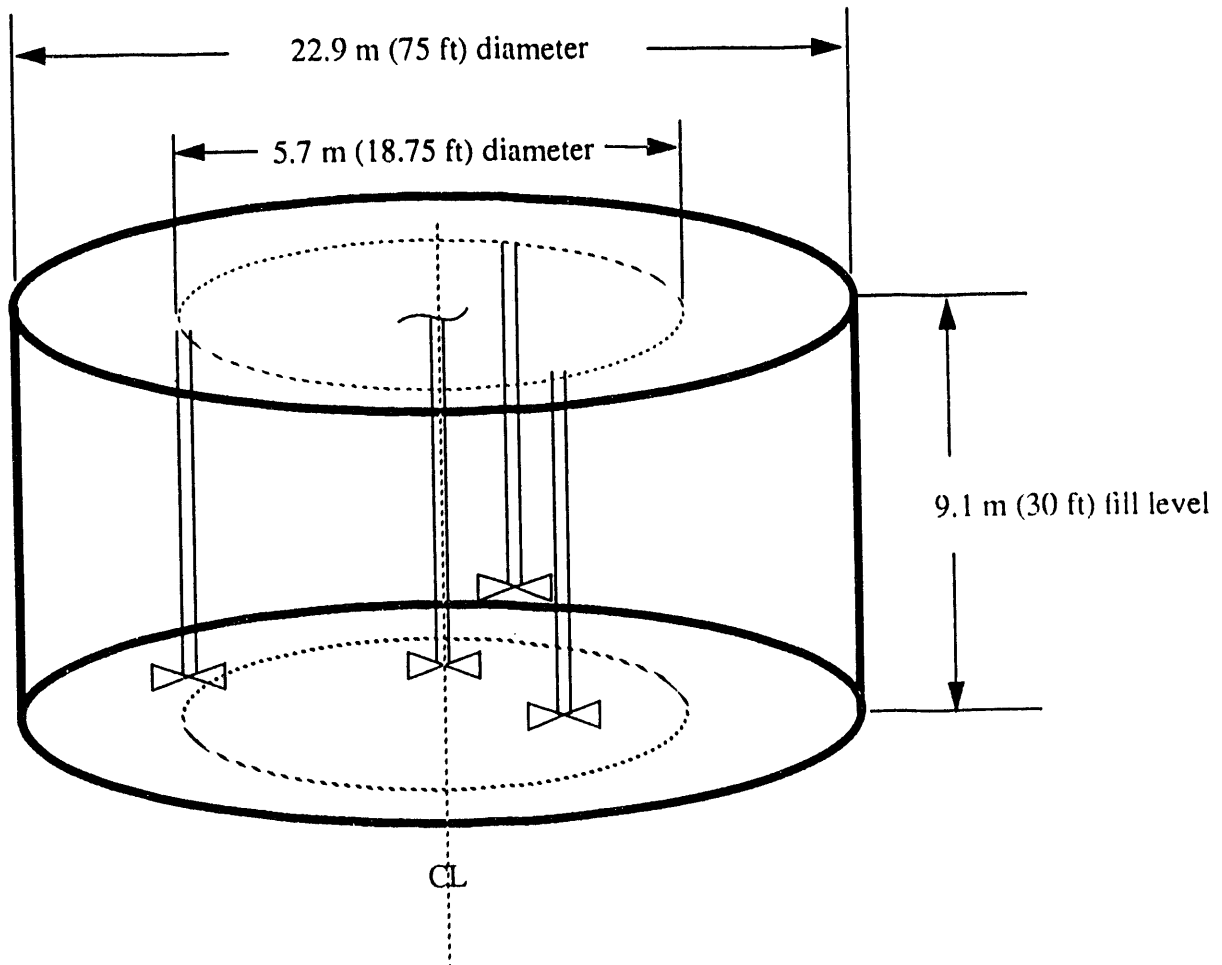


**FIGURE 5.7** Schematic of the Four-Pump Agitation System

conjunction with height of the jet above the floor, it would not be prudent to increase the nozzle centerline above the 0.46 m (1.5 ft) design location above the floor. Raising the nozzle further may cause the jet to be affected by fluid height at an even higher depth.

The retrieval pump inlet can be located to enhance the uniformity of the process feed withdrawn from the HWVP feed preparation tank. cursory investigations show that the pump inlet should be located below the mid-depth of the fluid.

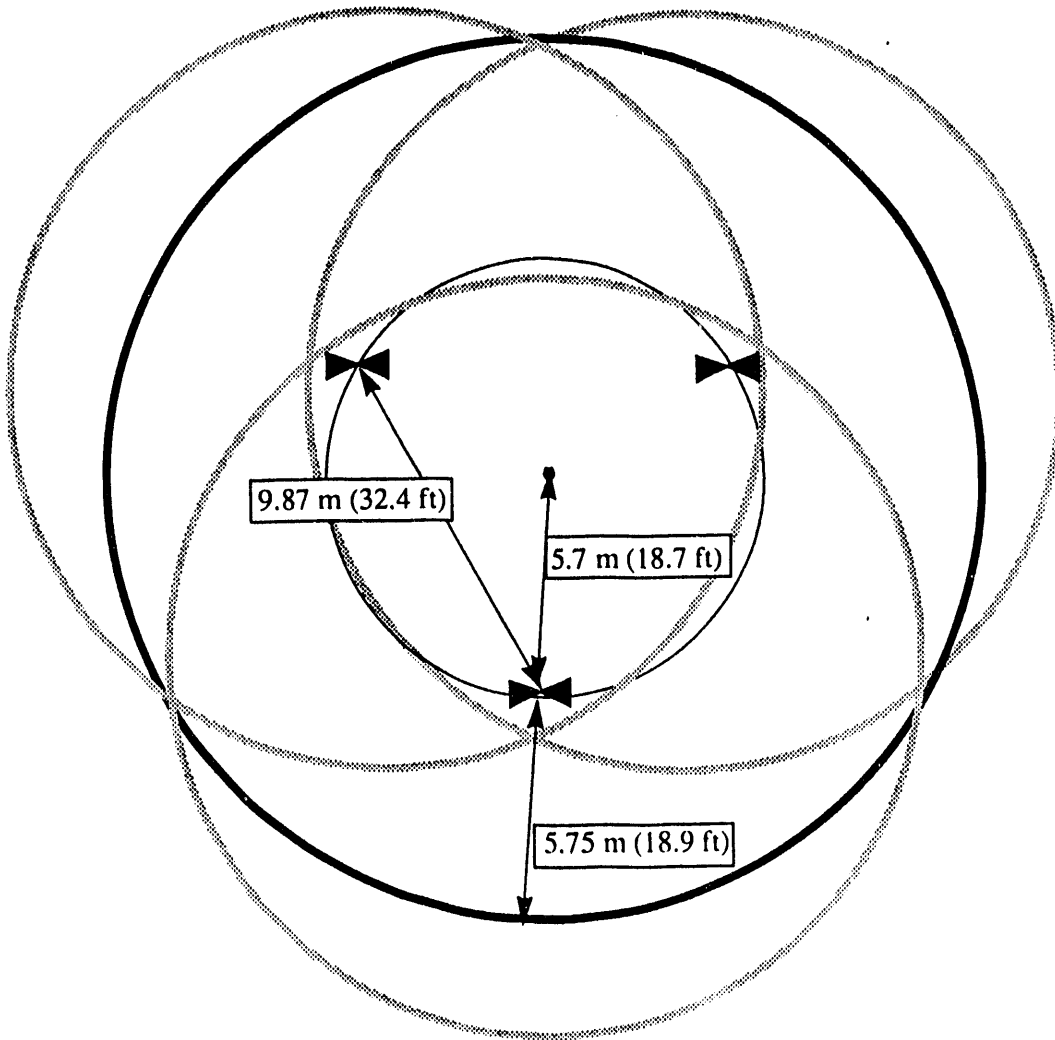


**FIGURE 5.8** Planar View of Four-Pump Configuration

### 5.2.3 Dynamic Parameters

Jet asynchronization should be implemented to ensure a random character to the resuspension of material from the tank floor. It is difficult to envision perfectly synchronized pumps; nevertheless this condition is probably not desirable because it would promote selective accumulation in areas where continued jet interferences occur. Such interferences may inhibit resuspension.

No additional specific recommendations for dynamic parameters are offered. As a part of the Double-Shell Tank Retrieval project, conducted by PNL for WHC, correlations will be developed to predict dynamic parameters required for sludge mobilization and maintaining slurry concentration uniformity (Bamberger, Liljegren, and Lowery 1993). These correlations will also be applicable for operation of the mixing pumps planned for use in the HWVP feed preparation tanks.

## REFERENCES

- Abraham, G. 1963. Jet Diffusion in Stagnant Ambient Fluid. Publication No. 29, Delft Hydraulics Laboratory. Waterloopkundig Laboratorium, PO Box 177, Delft, The Netherlands.
- Bamberger, J. A., L. M. Liljegren, and P. S. Lowery. 1993. Strategy Plan A Methodology to Predict the Uniformity of Double-Shell Tank Waste Slurries Based on Mixing Pump Operation. PNL-7665, Pacific Northwest Laboratory, Richland, Washington.
- CRC. 1975. Handbook of Chemistry and Physics. 56th ed. R. C. Weast, ed. CRC Press, Cleveland, Ohio, pp. D2.56-57.
- Dickey, D. A., and J. G. Fenic. 1976. "Dimensional Analysis for Fluid Agitation Systems." Chem. Eng. January 5, 1976, pp. 7-13.
- Fosset, H., and L. E. Prosser. 1949. "The Application of Free Jets to the Mixing of Fluids in Bulk." Proc. I. Mech. E. 160:224-251.
- Fox, E. A., and V. E. Gex. 1956. "Single-Phase Blending of Liquids." AICHE J. 2(4):539-544.
- Fromentin, A. 1989. Particle Resuspension from a Multi-Layer Deposit by Turbulent Flow. PhD Dissertation. Paul Scherrer Institut, Switzerland.
- Gates L. E., J. R. Morton, and P. L. Fondy. 1976. "Selecting Agitator Systems to Suspend Solids in Liquids." Chem. Eng. May 24, 1976, pp. 31-37.
- Korn, G. A. and T. M. Korn. 1968. Mathematical Handbook for Scientists and Engineers. Section 6.5-1, McGraw-Hill Book Company, New York.
- Kramers, H., G. M. Baars, and W. H. Knoll. 1953. Chem. Eng. Sci. 2:35.
- Marr, G. R. 1959. The Dynamical Behavior of Stirred Tanks. Ph.D. Thesis, Princeton University, Princeton, New Jersey.
- Marr, G. R., and E. F. Johnson. 1963. "The Pumping Capacity of Impellers in Stirred Tanks." AICHE J. 9(3):383-385.
- Norwood, K. W., and A. B. Metzner. 1960. "Flow Patterns and Mixing Rates in Agitated Vessels." AICHE J. 6(3):432-437.
- O'Brien, J., S. Julien, and Y. Pierre. 1988. "Laboratory analysis of Mudflow Properties." Journal of Hydraulic Engineering. Vol. 114, No. 8.
- Onishi, Y, D. Dummuller, and D. S. Trent. 1989. Preliminary Testing of Turbulence and Radionuclide Transport Modeling in the Deep-Ocean Environment. EPA 520/1-89-018, US Environmental Protection Agency, Washington, DC.

Onishi, Y., and D. S. Trent. 1985. "Three-dimensional Simulation of Flow, Salinity, and Radionuclide Movements in Hudson River Estuary." Proceedings of the Specialty Conference: Hydraulics and Hydrology in the Small Computer Age, HY Div. ASCE, Lake Buena Vista, Florida., August 12-17, 1985.

Onishi, Y., and D. S. Trent. 1982. Mathematical Simulation of Sediment and Radionuclide Transport in Estuaries. NUREG/CR-2423, PNL-4109, Pacific Northwest Laboratory, Richland, Washington.

Peterson, M. E., R. D. Scheele, and J. M. Tingey. 1989. Characterization of the First Core Sample of Neutralized Current Acie Waste from Double-Shell Tank 101-AZ. PNL-7758, Pacific Northwest Laboratory, Richland, Washington.

Rajaratnam, N. 1976. Developments in Water Science 5: Turbulent Jets. Elsevier Scientific Publishing Company, Amsterdam, The Netherlands.

Tatterson, G. B. 1991. Fluid Mixing and Gas Dispersion in Agitated Tanks, pp. 286-302, McGraw-Hill Book Company, Inc., New York.

Teeter, A. M. 1988. New Bedford Harbor Project -- Acushnet River Estuary Engineering Feasibility Study of Dredging and Dredged Material Disposal Alternatives -- Report 2. Sediment and Contaminant Hydraulic Transport Investigations. US Army Corps of Engineers, Waterways Experiment Station, Vicksburg, Mississippi.

Trent, D. S. and L. L. Eyler. 1992. TEMPEST A Computer Program for Three-Dimensional Time-Dependent Computational Fluid Dynamics, Volume 2, Input Instructions, Version T. Battelle Memorial Institute, Pacific Northwest Laboratory, Richland, WA.

Van de Vusse, J. G. 1955. "Mixing by Agitation of Miscible Liquids." Chem. Eng. Sci. 4:178-200.

Van de Vusse, J. G. 1962. "A New Model for the Stirred Tank Reactor." Chem. Eng. Sci. 17:507-521.

DISTRIBUTION

<u>No. of Copies</u>		<u>No. of Copies</u>	
2	DOE/Office of Scientific and Technical Information	30	<u>Pacific Northwest Laboratory</u> J. A. Bamberger, K7-15 (10) J. M. Bates, K7-15 I. G. Choi, K7-15 R. E. Dodge, K7-15 C. W. Enderlin, K7-15 L. L. Eyler, K7-15 L. K. Holton, P7-43 L. M. Liljegren, K7-15 N. J. Lombardo, K7-02 E. W. Pearson, K7-15 J. R. Phillips, K7-15 M. R. Powell, P7-19 P. A. Scott, P7-19 G. Terrones, K7-15 D. S. Trent, K7-15 Publishing Coordination Technical Report Files (5)
	<u>ONSITE</u>		
7	<u>DOE Richland Field Office</u>  S. D. Bradley, A5-10 M. Dev, A5-21 R. E. Gerton, A4-02 (2) P. E. Lamont, A5-14 (2) G. W. Rosenwald, A4-02		
20	<u>Westinghouse Hanford Company</u> D. G. Baide, G6-16 (5) J. R. Baker, G6-02 K. L. Engelhardt, G6-16 S. K. Farnsworth, H5-55 D. T. Heimberger, R2-07 B. A. Kendall, B4-66 W. C. Miller, S4-55 G. E. Stegen, G6-06 L. C. Stegen, R2-07 R. N. Wagner, G6-06 E. D. Waters, R2-07 B. A. Watrous, G6-08 Document Clearance Adm. (2) Project WE14 Files (2)		

**DATE  
FILMED**

8 / 20 / 93

**END**

